Title
STUDIES OF THE EVENTS OCCURRING AT GAS-EVOLVING ELECTRODES

Author
Putt, Ronald Alan.

Publication Date
1975-10-01

LBL-3989
c.1

STUDIES OF THE EVENTS OCCURRING AT GAS-EVOLVING ELECTRODES

Ronald Alan Putt
(M. S. thesis)

October 1975

Prepared for the U. S. Energy Research and Development Administration under Contract W-7405-ENG-48

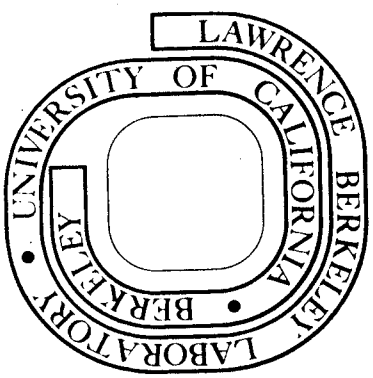

LBL-3989
c.1

DISCLAIMER

This is dedicated to
the music and memory of
Jim Croce

Table of Contents

STUDIES OF THE EVENTS OCCURRING AT GAS-EVOLVING ELECTRODES

Ronald Alan Putt

Inorganic Materials Research Division, Lawrence Berkeley Laboratory
and Department of Chemical Engineering; University of California
Berkeley, California

ABSTRACT

The physical events associated with the evolution of hydrogen and oxygen at electrode surfaces in concentrated sulfuric acid and potassium hydroxide solutions have been observed, and recorded by flash photography. A special technique for photographing the electrode surface shortly after current initiation (13-300 m sec) provided a view unobstructed by rising gas bubbles. Bubble growth rate, number density, and maximum bubble size data were obtained for gas generation rates in the range 3.5-14 cm^3/cm^2 min, corresponding to current densities for hydrogen evolution of .5-2a/cm. The velocity of the rising gas emulsion and degree of gas bubble coalescence within it were also observed.

The growth characteristics of bubbles depend strongly on the electrolyte composition, different for hydrogen and oxygen in the same electrolyte. In the range studied, increasing the gas generation rate does not change the character of the events, only the rate of their occurrance. Bubble growth before separation involves repeated sequences of coalescences.

Comparison of estimates of the sizes that bubbles should reach under equilibrium growth conditions with those observed reveals that separation is controlled by the dynamics of bubble interactions.

Altering the surface condition of the electrode showed that the microscopic roughness of a planar electrode has little effect on the character of gas evolution. The electrolyte velocity generated by the rising gas bubble stream is primarily a function of gas generation rate and is not overly dependent on the character of gas evolution. An extreme sweeping action, or "scavenging effect", of gas bubbles rising along the electrode surface occurs extensively in sulfuric acid electrolyte.

I. INTRODUCTION

Electrolytic evolution of gases is of great industrial importance. Of the many processes in which gas evolution occurs at one or both electrodes, the manufacture of chlorine and hydrogen have gained greatest economic significance. Despite its widespread applications, electrolytic gas evolution has received relatively little attention in scientific circles. Chemists have solely concentrated on over-voltage phenomena associated with the charge transfer reactions, while chemical engineers have been primarily concerned with practical improvements of cell and electrode design. Even a crude qualitative discussion of what occurs when bubbles form and grow on an electrode surface is lacking in nearly all textbooks and monographs on electrochemistry or electrochemical technology. A review of the scientific and technological literature reveals only sporadic and at that, quite recent efforts concerning the elucidation of the intriguingly complex events occurring at electrode surfaces when a gas phase is generated. This lack of significant research efforts directed toward understanding the dynamics of electrolytic gas evolution is even more surprising if one considers its close resemblance to nucleate boiling.

Certain key problems associated with electrolytic gas evolution can be easily identified;

1. Because of gas holdup in the interelectrode space the effective electrolyte resistance is larger than in the absence of bubbles.

2. Bubbles attached to the surface shield it, and consequently the actual current density is larger than it would be on the free surface. The flow of current through the reduced cross section manifests itself in an increased ohmic voltage drop.
3. Significant concentration overpotential is caused by the supersaturation of gases at the electrode surface.

In 1967 Cheh[1] conducted a theoretical treatment of the phenomena associated with gas evolution. Specifically he analyzed bubble nucleation, bubble growth for various symmetries and initial dissolved gas concentration fields, bubble separation, and growth rates of rising bubbles. Considering only the dynamics of single, isolated gas bubbles in spherical and axisymmetric geometries, he did not extend his theoretical treatment to the effects of bubble interactions on bubble growth and separation. Although his analysis provides insight to certain details of the bubble growth process, clearly the "real" situation at a gas-evolving electrode involves significant effects related to such interactions of bubbles. Because the simultaneous and consecutive events occurring during the evolution of gases at electrode surfaces are quite involved, it is unlikely that an accurate analytical description of electrolytic gas evolution processes can be developed in the foreseeable future.

The purpose of the present study is to extend our understanding of the physical events occurring in the evolution of gases from electrode surfaces. The choices of electrode material, electrolyte composition, and gas generation rates (cm^3/cm^2 min.) were made to conform as much

as possible to industrially important conditions. Bubble nucleation site densities and distributions, bubble growth rates and number densities, and terminal bubble sizes on the electrode surface are measured, and observations are made of the events taking place after bubbles separate from the surface.

A special experimental technique was employed to allow observation of the events on the surface as bubbles nucleate, grow, coalesce, and eventually separate. Since in steady state electrolysis the view of the surface is blocked by bubbles rising in the electrolyte, the electrode was photographed very short times after switching on the current, before rising bubbles block the view of the electrode surface. In this manner the incipient events of gas evolution could be observed up to the time when the first layer of bubbles separated. Although the dissolved gas concentration and electrolyte velocity do not reach their steady state profiles during these short time periods (less than 1 sec.), the information gained during this "incipient bubble evolution" period provides valuable insight to the events occurring on the electrode surface at steady state.

II. LITERATURE REVIEW

In 1933 Kabanov and Frumkin[2] presented an analytical treatment of the factors influencing the size of electrolytically generated gas bubbles. They offered an alternate explanation of the observations made by Coehn and Neumann[3,4] on gas bubble sizes at separation. Coehn et al.'s observations were as follows;[1]

1. In alkaline solutions small bubbles were formed at the cathode and large bubbles were formed at the anode.
2. In sulfuric acid solutions the reverse occurred.
3. In sulfuric acid solutions the bubble size was dependent on the acid concentration.
4. In all cases the bubble sizes at separation were proportional to the current density.

Coehn and Neumann attempted to explain these phenomena through electrostatic attraction and repulsion between the supposedly charged bubbles and the surface of the electrode. Kabanov and Frumkin presented calculations to show that, based on estimates of the magnitude of the charges on the bubbles, the electrostatic forces were about six orders of magnitude smaller than the hydrostatic forces present. Instead they proposed that the bubble size at disengagement is determined by the vertical component of the surface tension forces, which depends on the contact angle the bubble makes with the surface of the electrode. They backed up their arguments with measurements of bubble sizes that agreed well with their predictions. Working at very low current

densities ($.5\text{-}5\times10^{-4}$ a/cm^2) their typical bubble growth times were as long as 15 hours, which allowed equilibrium of the opposing forces to exist. Furthur, all their observations were of horizontal electrodes facing upward. Mercury, platinum, and silver were used as electrode materials. The point of detachment of the bubbles was found to be when the following equality was reached: $V\rho g = (2/3)\pi a\sigma\sin\theta$, where V is the bubble volume, ρ the bubble density, g the acceleration due to gravity, a the perimeter of adhesion of the bubble, σ the surface tension of the solution, and θ the contact angle of the bubble measured through the liquid. Also they showed that the breakoff diameters followed a similar curve with electrode potential as did the electrocapillarity curves, and they suggested that the effect of potential on the surface tension of the liquid was the major contributing factor in the observed variation of bubble size with current density (i.e. electrode potential).

Clark, Strenge, and Westwater[5] attempted in 1957 to obtain evidence as to the identity of active sites in nucleate boiling. They conducted nucleate boiling studies of ether and pentane at a prepared metal surface which was submerged in the test liquid. The metals studied were zinc and an aluminum alloy. Their direction was to seek differences in the boiling characteristics brought about by morphological variations in the heated surface. No differences were observed in the boiling curves for polycrystalline metals and single crystal metals at various crystallographic orientations. The nucleation sites were observed to consist of pits and scratches in the metal surface, with no preferential nucleation at grain boundaries. Electron micrographs of the surfaces

showed that regardless of the care taken in polishing, including use of fine aluminum oxide and even electropolishing, there still remained tiny pits in the surface, and the most active nucleation sites were pits having diameters of 8-80 microns. They also recorded the heat flux variation to the metal surface with time and found it to be of an unsteady, cyclic nature, indicating that the events of bubble nucleation, growth, and separation had a measureable effect on the heat transfer rate at the surface.

Kellogg,[6] in order to gain insight to the "anode effect" in the aluminum process, conducted water electrolysis at very high voltages in order to study the analog of this effect in aqueous solutions. He used a platinum wire dipped into a large beaker of either sulfuric acid solution or sodium hydroxide solution as the working electrode and a platinum sheet dipped in the same electrolyte as the counter electrode. He also fashioned a steel alloy tube of small diameter with a thermocouple soldered in the tip as another working electrode to follow electrode temperature. In his experimental procedure he increased the cell voltage through the water electrolysis regime, recording current as a function of voltage. In this regime the bubbles would nucleate, grow and separate regularly and the current was roughly proportional to the applied voltage. Then, at a certain voltage, which in all cases corresponded to the point at which the electrode temperature reached 100C, the current reached a plateau where furthur increases in voltage did little to increase the current. The photographs taken in this

"transition region" showed that the bubble evolution characteristics were altered such that contiguous gas sheaths surrounded the electrode and the liquid made contact with the hot electrode only briefly and at distinct points. Furthur voltage increases past a specific value (ca. 60V) resulted in the current dropping from a typical value of 6 amps (electrode active area approximately 0.31 cm^2) at 25 volts in the transition region to a lower value of about 1 amp in a new region called the "aqueous anode effect" region. Furthur voltage increases in this region produced a slight decrease in the cell current. Electrode temperatures in this region ranged from 165-620C, and at high voltages the platinum electrode tip could be seen to glow red. The photographs of the electrolysis under these conditions showed a continuous vapor blanket or sheath around the electrode. However, the finite cell current meant that there was a faradaic reaction occurring and analysis of the evolved gas showed it to be oxygen or hydrogen, depending on the polarity of the working electrode. Since the liquid was not in contact with the electrode at any point, it was proposed that the faradaic reaction was occurring at the vapor-liquid interface, and that the current was carried across the vapor space by the migration of the charged ions produced by ionization of the vapor itself. Thus the vapor blanket or sheath around the electrode was being maintained by the vaporization of the liquid at or near the very hot electrode.

Scriven,[7] in what is considered a classical work in the subject, set forth a mathematical treatment of the process of spherically symmetrical growth of a single hemispherical gas or vapor bubble in a

semi-infinite liquid, for the case in which the phase growth is controlled by the rate of heat transfer (for the case of boiling) or mass transfer (for the case of electrolytic gas evolution) to the surface of the bubble. This he termed the asymptotic growth period of the vapor phase, in contrast to the short time period surrounding nucleation and intitial growth of the bubble in which surface forces and inertial effects are dominant. Furthur assumtions made to simplify the mathematics included constant physical properties of the gas (vapor) and liquid, heat or mass flow only by conduction or diffusion, and that the viscous dissipation terms in the equation of motion are negligible. He formulated the solution for the dependence of the bubble radius with time through the equation $R=2\beta\sqrt{\mathcal{D}\theta}$ (for the case of mass transfer and electrolytic gas evolution), where R is the bubble radius, β is the "growth constant", a function of the physical properties of the liquid and gas and the degree of supersaturation, $\mathcal{D}$ is the diffusion coefficient, and θ is time.

Westerheide and Westwater,[8] in 1960, studied the growth of individual gas bubbles generated electrolytically under isothermal conditions as an experimental extension of Scriven's work. Their system was a polished platinum micro-electrode, at which hydrogen was generated from .1 and 1 N sulfuric acid solutions at low current densities (.1 and .2a/cm^2). The growing bubbles were photographed with a high speed (400-2400 frames per second) motion picture camera, after which the film was developed, and studied on a motion picture analyzer.

By measuring the bubble growth rates they determined values of β, the growth constant in the equation $R=2\beta\sqrt{D\theta}$, then made use of computer-generated plots of

$$\phi = \left(\frac{\rho_L}{\rho_g}\right)\left(\frac{C_\infty - C_{sat}}{\rho_L - C_{sat}}\right) \quad \text{vs.} \quad \beta$$

for various

$$\varepsilon = \frac{\rho_L - \rho_g}{\rho_L} ,$$

as developed by Scriven, to determine the degree of supersaturation. The bubble growth curves closely followed the $\sqrt{\theta}$ dependence predicted by the equations. From their calculations it was found that the degree of supersaturation of dissolved hydrogen gas in the solutions varied in the range 8-24 times the saturation concentration, depending on the current density. It should be noted that these results were obtained for single bubbles growing without the influence of any neighboring bubbles. Occasionally their photographs showed two bubbles growing side by side and eventually coalescing. Their attempts to mathematically model the growth through coalescence were in vain; the reason for this was reported to be that spherical symmetry does not exist in the dissolved gas concentration profile immediately after coalescence. Furthur they found that bubbles growing close to one another deviated in their growth both above and below the $\sqrt{\theta}$ dependence predicted. Interesting phenomena of bubbles bouncing back to the surface after coalescence and bubbles sliding along the surface during growth were also observed.

Ibl[9] studied the mass transport aspects of gas-evolving electrodes through measurement of the rate of redox couple reactions (e.g. Fe^{++}-Fe^{+3}) occurring at their limiting currents with gas evolution taking place simultaneously. For hydrogen evolution in sulfuric acid solutions Ibl obtained a correlation of the mass transfer coefficient to the rate of gas being evolved, in the form $K_L \sim V^{1/2}$, where K_L is the mass transfer coefficient (cm /min.) and V is the gas evolution rate (cm^3/cm^2 min). He proposed a "surface renewal" model in which fresh solution of bulk reactant concentration is brought to the surface of the electrode each time a bubble detaches and leaves the surface. The mass transfer process to or from the electrode is thus a non-steady state diffusion inside this initially uniform volume of liquid. The overall mass transfer rate is then determined as a time average of the unsteady state rate over the nominal time period which elapses between successive bubbles at a given site. Intuitively the observed dependence of mass transfer coefficient on rate of gas evolution is explained by the fact that more bubbles are generated in a given electrode surface area per unit time, and fresh, bulk solution is brought to the surface more frequently.

Glas and Westwater[10] made furthur use of the micro-electrode concept and high speed motion picture photography in their study of bubble growth in electrolytic gas evolution. Studying the growth of hydrogen, oxygen, chlorine, and carbon dioxide at highly polished platinum, nickel, copper, and iron electrodes, they limited their current densities to .01-.12 a/cm^2 and varied the system pressure from

one to two atmospheres. Extensive measurements were made of contact angles and growth curves. From the latter they calculated the amount of supersaturation of the dissolved gas in the solution for each of the gases studied. These values are as follows:[3]

$1.54\text{-}19.9X$ for H_2

$1.36\text{-}15.4X$ for O_2

$1.08\text{-}1.64X$ for CO_2

$1.018\text{-}1.324X$ for Cl_2

From their photographs they determined that the early growth period during which the surface forces and inertial effects are important, i.e., the time period between nucleation and Scriven's "asymptotic growth" stage, was on the order of .6 msec. They furthur attempted to relate β, the growth coefficient, to the current density, using both a steady state model and an unsteady state model. In their steady state model they proposed the relationship $\beta=K_I I^{1/3}$, where I is the current density and K_I is an empirically determined constant. The unsteady state model incorporated a waiting time τ prior to bubble growth, during which the concentration profile develops with time as given by the error function relationship. The wide scatter in their plots of β vs I was explained by the supposedly great variation in waiting times from one bubble to the next. By using fewer nucleation sites in their analysis they were able to eliminate much of the scatter, and found that the steady state model was better able to describe the results for hydrogen evolution at platinum, whereas for oxygen and chlorine evolution the unsteady state model was better. For carbon

dioxide evolution both models worked equally well. From observations of many bubbles issuing from the same site they determined that the events were not identical from one bubble to the next; sizes and growth curves varied about a mean value. By varying the electrode metal for hydrogen evolution they observed that the growth coefficient was not a function of the electrode material, despite the fact that the hydrogen overpotential varies from metal to metal. However, the initial growth rate of the bubbles varied from one metal to the next, it being the fastest for the nickel electrode. Their explanation for this was that nickel, being the hardest, had a different surface morphology than the others after polishing, and this was somehow related to the rate of initiation of bubble growth. An estimate of the size of a "large" nucleation site was given as 5 microns. Other observations made were that the very smooth electrode surfaces increased the waiting times for bubble nucleation and by contact angle made by the bubbles with the metal surface decreased with growth, although it had little effect on the growth coefficient.

Buehl and Westwater[11] extended Scriven's treatment by relaxing some of the assumptions made by him. Specifically they allowed for the contact angle to be other than 90°, they included the effect of the wall, and they allowed fluid velocities in other than a purely radial direction (note that these necessarily also invalidate the assumption of spherical symmetry). Using computer techniques to solve the resulting coupled partial differential equations, they showed that for a variation in the contact angle from 0-90° the bubble growth

rate changed only 30% at most, and furthur that for fast bubble growth the concentration gradient existed only in a very thin shell around the bubble.

Landolt et al.[12] studied hydrogen evolution at the cathode of a cell in a flow channel under ECM (electrochemical machining) conditions, specifically high current densities and high flow rates of electrolyte. The electrodes were copper and the electrolyte was 2N KCL. Their general observation was that the bubble size decreases with increased flow rate and increases with increasing current density. Specifically they found that above 7800 cm/sec all bubbles are below 20 microns in diameter, the resolution limit of the optics employed. They were able to justify the decrease in bubble size with increased flow rate, based on a previously-formulated model, but the increase in size with current density left them somewhat puzzled. They were also disturbed by the wide distribution of bubble diameters observed at low current densities.

Bon's work[13] involved measuring the supersaturation of dissolved gas at a gas-evolving electrode. Bon used bright and platinized platinum cathodes mounted horizontally and facing upward to generate hydrogen from 1 and 2M sulfuric acid solutions. Measurements of the degree of hydrogen supersaturation in the vicinity of the cathode were performed in a novel manner; 8 very thin (6 micron) platinum ring reference electrodes were placed around the circumference of the cathode at very small vertical distances from the face of the cathode by stacking them one atop the other with very thin sheets of plastic

between them acting as insulators. The reference hydrogen electrode and the counter electrode were in separate compartments, connected via electrolyte bridges. Steady state electrolysis was established, and then the current was interrupted to eliminate the IR voltage drop. A digital scanner then recorded the ring reference electrode voltages very 30 msec against the remote hydrogen reference electrode. Plotting the potential of each ring electrode with time and extrapolating to the instant of interruption of current provided the steady state voltage profile, which is related to the hydrogen supersaturation through the Nernst equation. In order to test the surface renewal model of Ibl,[9] Bon needed to measure the bubble size distributions above the cathode. In doing so he found an average diameter of 40 microns for 2.5 and 25 ma./cm^2 and 80 microns for 250 ma./cm^2, and also that the bubbles grew little if any during rise. The results of his supersaturation measurements, which typically showed hydrogen supersaturation of 100 atm at the electrode surface for a current density of 100 ma./cm^2, were basically in agreement with that predicted by Ibl's model.[9]

Janssen and Hoogland[14] sought to determine the effect of the current density and electrode height on δ_N, the Nernst boundary layer thickness for mass transfer, at a gas-evolving electrode. Furthur they observed the nucleation site distribution, bubble trajectories, and bubble coalescence phenomena associated with electrolytic gas evolution. Their test electrodes were vertical platinum sheets of heights ranging from 1-16 mm, at which they studied hydrogen, oxygen, and chlorine evolution

with still photography and high speed motion picture photography. In a manner similar to Ibl's[9] they also measured the apparent boundary layer thicknesses. They found that δ_N decreases with increasing current density in the range 6-1000 ma./cm^2. Furthur they presented a qualitative picture of the events occurring at the electrode surface during gas evolution, but they were restricted in this to below 150 ma./cm^2, as the view of the surface was blocked at higher current densities by the rising bubbles. The results of the measurements prompted them to dispute the validity of Ibl's surface renewal model, and in its place they proposed a "hydrodynamic" model, in which mass transport to the electrode surface is primarily due to the electrolyte flow upward along the electrode surface produced as a result of the rising bubbles. In fact, their measured values nearly coincided with the optically measured distances between the rising bubbles and the surface of the electrode.

Janssen and Hoogland,[15] in a continuation of their previous work,[14] extended their measurements of δ_N and its variation with current densities to alkaline as well as acid solutions and for horizontal as well as vertical electrodes. Since their results from the previous publication were not entirely in accord with those of Ibl and Venczel, they sought to study the effect of polishing the electrodes with Viennese lime, a practice of Ibl and Venczel.[16] They found that irregular results were obtained with unpolished electrodes but regular results were obtained with polished electrodes. The orientation of the electrode was found to have little effect on the measured δ_N values.

Furthur, the results of the δ_N measurements here also repudiated Ibl's surface renewal model, and reinforced their interest in the hydrodynamic model of mass transport at gas-evolving electrodes discussed in their previous work.[14]

Venczel[17] employed a transparent electrode, formed by high vacuum deposition of a metal film on a glass plate, to perform optical studies of gas bubble formation at electrode surfaces. With this apparatus he was able to observe in detail the events occurring right at the surface. Platinum, chromium, nickel, and gold were studied with this technique; hydrogen bubbles were generated from sulfuric acid solutions at current densities of 10-250 ma./cm^2. His results are summarized as follows:

1. the gas bubble sizes varied from barely visible to several millimeters in diameter.
2. In general the bubble size was smaller for the addition of various organic "Inhibitors".
3. The bubble size was observed to vary with the type of electrode metal used.
4. One type of coalescence observed was in which a bubble slid upward slowly along the surface, gathering bubbles and leaving behind a bubble-free path.
5. Uniform growth and surface coalescence occurred on platinum and graphite electrodes, and uneven growth took place, with the bubbles separating before coalescence could occur, at iron and copper electrodes (note that solid metal electrodes

of these materials were also used for the observations, in which the optical objective was in front of the surface).

6. In the vicinity of a large bubble other sites were active, but after its detachment their activity decreased; he attributed this phenomenon to an increased actual current density when the larger bubble was still on the electrode.
7. There was observed a definite liquid layer under the contact area of the bubble. The strength of adhesion of the bubble on the surface was related to the thinness of this layer, which in turn is a function of the metal wettability.
8. The degree of coverage of the electrode surface by the attached bubbles rose rapidly with current density up to about 25%, after which it remained constant despite furthur increases in the current density.
9. The bubble size was observed to decrease in the range .5 to .1 mm for current density increases of 10-250 ma./cm^2, above which it remained constant with current density.
10. Actual residence times of the bubbles on the surface were measured; these times ranged from .029 sec. for graphite at 500 ma./cm^2 to 10 sec. for platinum at 5 ma./cm^2.

In 1970 Ibl and Venczel[16] reported measurements of the mass transport rates at gas -evolving electrodes, wherein copper, nickel, and iron electrodes of 1 cm×1 cm were employed for hydrogen evolution from sulfuric acid solutions. Bubble size and residence time measurements were also performed to provide input to their mathematical models

of the processes occurring. They proposed two possible mechanisms for mass transport at a gas-evolving electrode;

1. "Rising Effect" - the stirring is caused by the flow of electrolyte upward along the electrode surface due to the rising bubbles.
2. "Detachment Effect" - The stirring is effected by the bubbles growing and detaching from the surface, in that the liquid is pushed away by the bubble as it grows, and then flows back to the surface when the bubble detaches.

Favoring the latter, they proceeded to develop a mathematical model which produced the following equations:

$$K_L = \sqrt{\frac{6DV(1-\theta)}{\pi R}}$$

$$\delta_N = \sqrt{\frac{\pi DR}{6V(1-\theta)}}$$

where V is the rate of gas evolution (cm^3/cm^2 sec), D is the diffusion coefficient (cm^2/sec), R is the bubble radius (cm), θ is the fraction of surface coverage by the bubbles, K_L is the mass transfer coefficient (cm/sec), and δ_N is the effective Nernst mass transfer boundary layer thickness (cm). Typical values for these are (for a platinum electrode in sulfuric acid at 250 ma./cm^2) R=0.15 mm, θ=.24, D=5.4×10^{-6} cm^2/sec., and δ_N = 0.0136 mm. An extremely thin boundary layer thickness of δ_N = 0.003 mm was measured for a current density of 2 a/cm^2.

In 1971 Ibl[18] surveyed the various aspects of the theory of electrolytic gas evolution. He described nucleation sites as geometric irregularities such as crevices, in which a gas pocket remains behind after bubble separation and acts as a bubble formation nucleus, these sites having typical dimensions of 5 microns. Bubble growth was proposed to consist of two stages, a very rapid initial stage where surface tension plays an important role and a second, slower stage in which mass transport of dissolved gas to the bubble surface from the surrounding liquid is the rate-determining step. The coalescence of two bubbles would occur when they grew to within a certain distance of one another. The force balance involved in determining the exact moment of bubble separation was discussed, however, only for the case of a horizontal electrode facing upward. He cited an equation, applicable for contact angles of less than 140°, which specifies the maximum bubble volume an attached bubble can attain;

$$V_{max} = \left(\frac{3}{\pi}\right)^3 \left(\frac{\gamma_1}{\rho_g}\right)^{3/2} \theta^3$$

where γ_1 is the gas-solution surface tension, ρ is the solution density, and g is the acceleration due to gravity. Concerning the current density dependence of bubble size, it was stated that at practical rates of gas evolution the forces involved are not at their equilibrium values and thus the bubble size may vary with current density, i.e., the rate of bubble production. In addition, the effects of the presence of neighboring bubbles and the hydrodynamic flow caused by the rising bubble stream were mentioned as contributors to the separation size of the bubble.

Darby and Haque[19] showed evidence that the combination of atomic to molecular hydrogen at the surface of the electrode could be the rate determining step vice the mass transport of the gas to the bubble. They employed high speed motion pictures of growing bubbles in conjunction with the instantaneous current traces recorded during the bubble growth to show that this could be the case under certain experimental conditions.

III. EXPERIMENTAL

A. Electrode Preparation

A half-inch diameter nickel rod of high purity* was machined to size and encased in epoxy** to electrically insulate the areas not to be used as active electrode surface. The end of the rod was hand finished with 1/0 grit emery cloth, using kerosene as lubricant, to obtain a flat but visibly scratched surface. For the trials requiring a very smooth surface the electrode surface was sequentially finished with increasingly fine grit emery cloth, with soap and water and alcohol rinse between stages. After the 4/0 grit treatment and rinse the electrode was then polished on a power wheel with first a 1 micron diamond paste in kerosene lubricant and then with .05 micron aluminum oxide paste with water as lubricant, again rinsing between stages with soap and water and alcohol. The final finish was mirror-like, having no scratches visible to the naked eye. Surfanalysis*** traces are shown in Fig. 1 as a comparison between the 1/0 (rough) surface and the .05 micron (smooth) surface profiles. Analysis of these traces showed that the 1/0 grit surface had an actual surface area exceding the geometric surface area by only 7%. After the surface finishing the electrode was rinsed with hot, soapy water, cleaned ultrasonically in acetone for 1-2 minutes, then pre-electrolyzed cathodically and anodically in 5M KOH at 1-2 a/cm^2 for at least 15 minutes each prior

---

*99.5% pure nickel rod, ORION CHEMICAL COMPANY

**SHELL 826 casting epoxy

***CLEVITE-GOULD Surfanalyzer Model 150

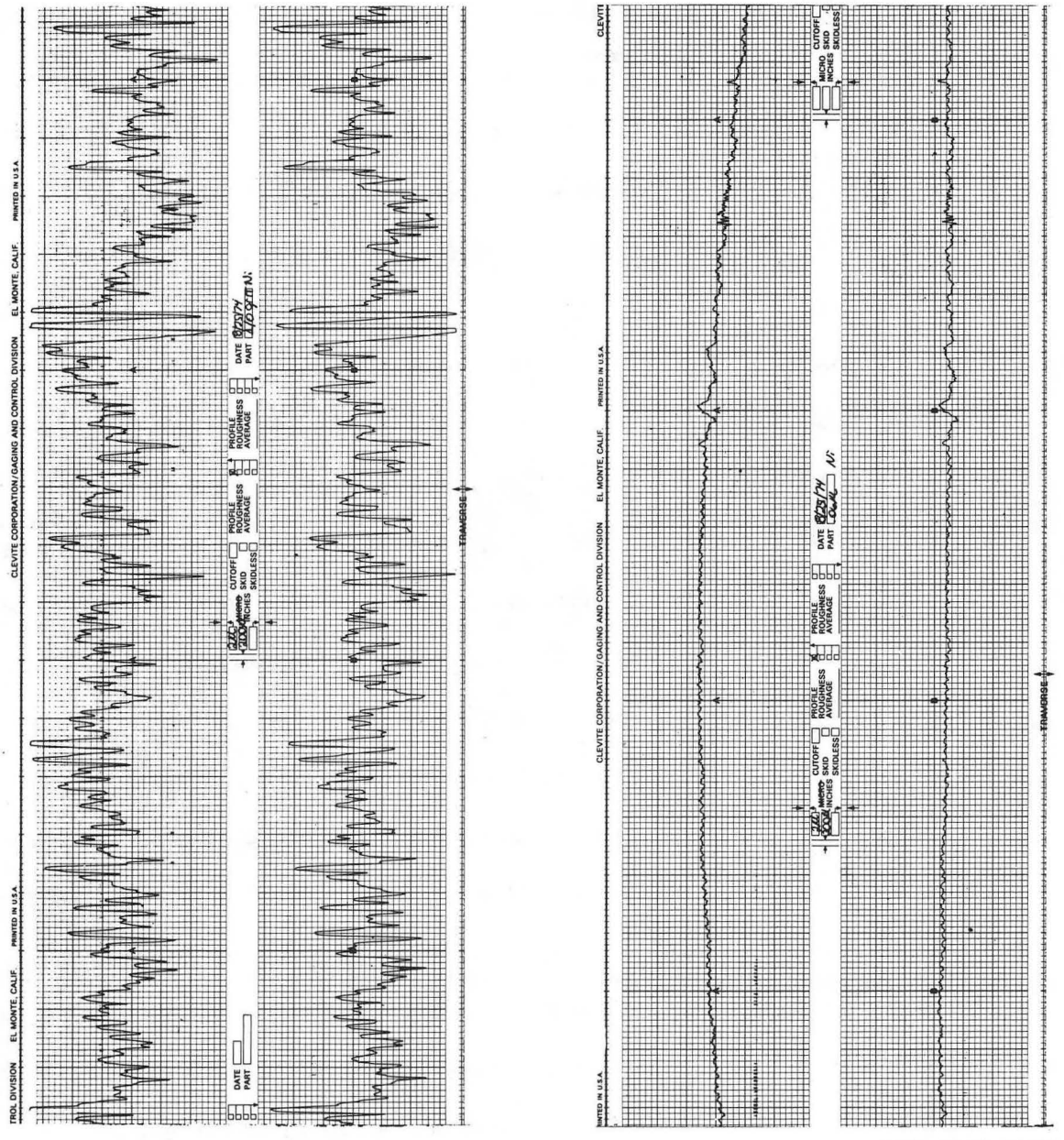

XBB 758-6368

(a) 1/0 grit

(b) 0.5 micron Al_2O_3

Fig. 1. Surfanalysis traces of 1/0 grit and 0.05 micron Al_2O_3 nickel electrode surface profiles.

to use in the bubble size experiments. This pre-treatment resulted in excellent reproducibility of experimental results.

B. Optics

The range of bubble diameters studied required magnification for proper observation. A BAUSCH AND LOMB microscope having a magnification of 13X was employed. The microscope was fitted with a camera attachment, which also provided via a beam-splitting prism an eyepiece mounted at a 90° angle from the optical axis for simultaneous viewing. This permitted focussing with the camera in place. The camera, a KODAK Colorsnap 35 using 35 mm KODAK Tri-X film, recorded the events taking place. The shutter had a variable speed of up to 1/200 sec and also a position for open-shutter photographs. The flash was provided by a Microflash Unit,* having a peak light output of 50×10^6 beam candlepower and a light time of 0.5 microseconds. Such a short light time was required to freeze the motion of the bubbles at the electrode surface, so that sharp, unblurred photographs could be obtained. The microflash was used with the open-shutter mode of the camera for the incipient growth and freely rising stream studies. For measurement of the speeds of rising bubbles the 1/200 second shutter speed was used and a high intensity incandescent lamp provided continuous illumination.

---

*EG & G 549 Microflash System

Analysis of the 35 mm negatives was performed by projecting them onto a 2×3 ft. screen in order to obtain furthur magnification for greater accuracy in size measurement. A draftsman's rule was used to measure distances. Multiplying the subject-to-negative magnification and negative-to-screen magnification provided the necessary conversion factor between measured and actual distances.

C. Incipient Bubble Growth Studies

Figure 2 shows the cell and electrode construction. Figure 3 is a photograph of the cell, optics, and lighting assembled for incipient bubble growth studies. The cell block, made of Lucite, is 7.5 cm high by 5 cm wide by 5 cm breadth. Opposite walls were bored out along a common axis to accommodate the electrodes. A round side window of pyrex glass was installed at an angle to provide an entrance for the light. The working electrode, a circular cylindrical rod 5 cm long, was encased in epoxy to electrically isolate the sides. In this epoxy an O-ring groove was cut, and an O-ring between the epoxy and cell block hole provided a water-tight seal. The counter electrode was machined from nickel pipe and cast in epoxy, with an O-ring also forming the water-tight seal between epoxy and the cell block hole on the opposite wall. Through the center of the epoxy a 1.3 cm hole, was drilled, and into the end face another pyrex window was set. This provided an optical path which allowed viewing the working electrode surface from its normal direction. The trigger circuit show in Fig. 4 provided via one pushbutton switch the capability of connecting the power supply to the cell instantaneously and sending a trigger pulse

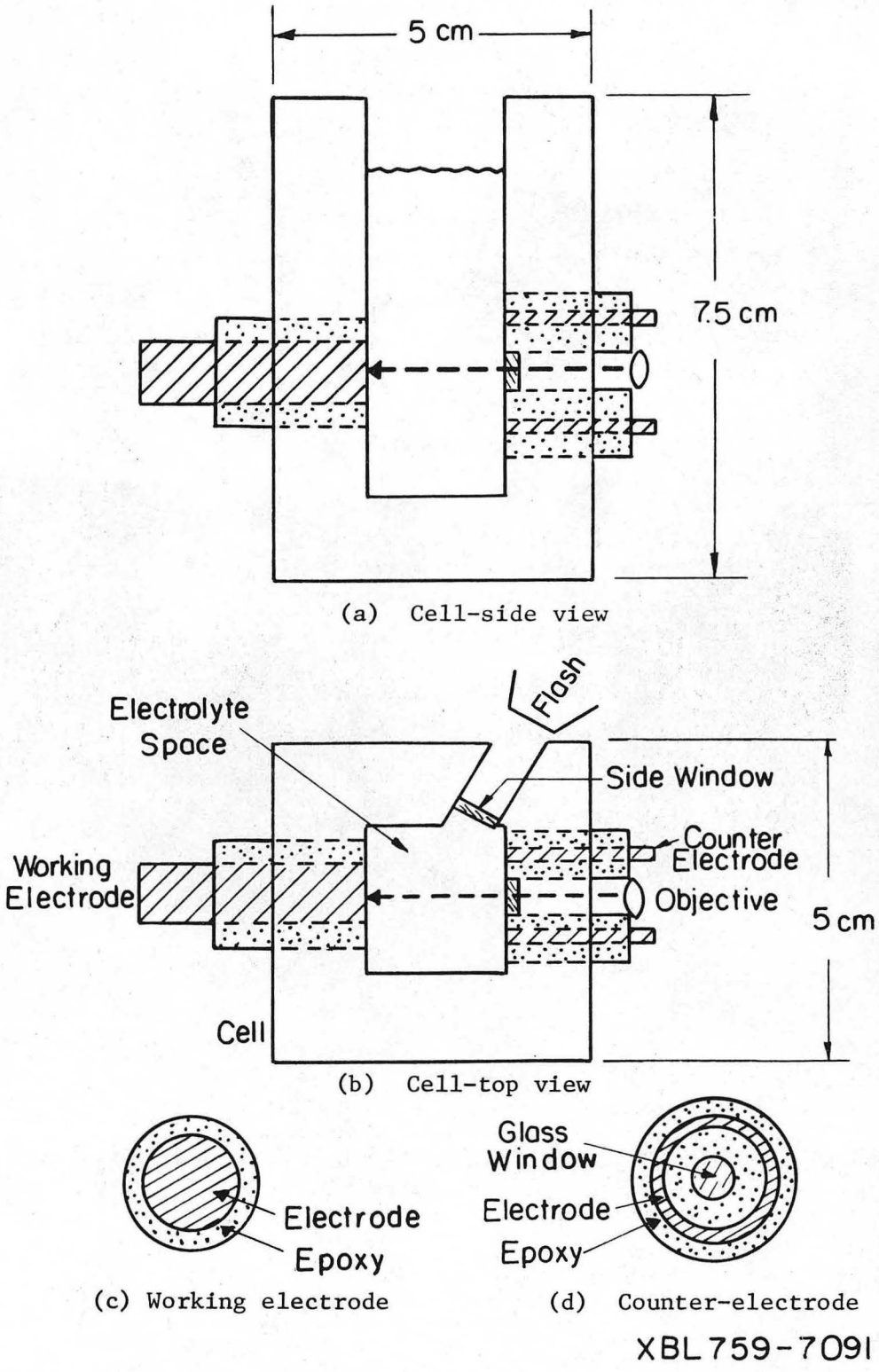

Fig. 2. Incipient bubble growth cell and electrode construction.

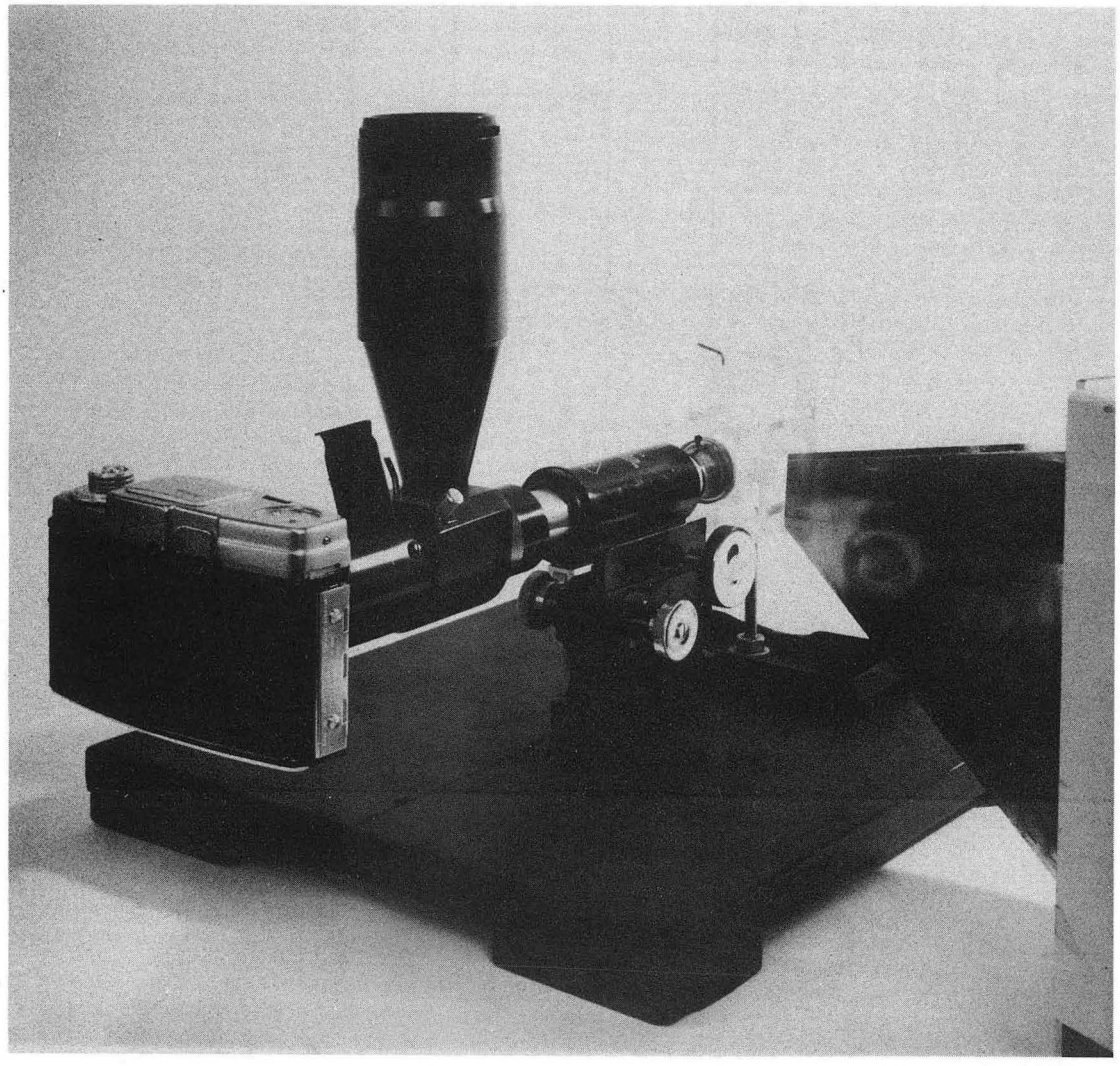

XBB 758-6025

Fig. 3. Assembled incipient bubble growth cell and optical apparatus.

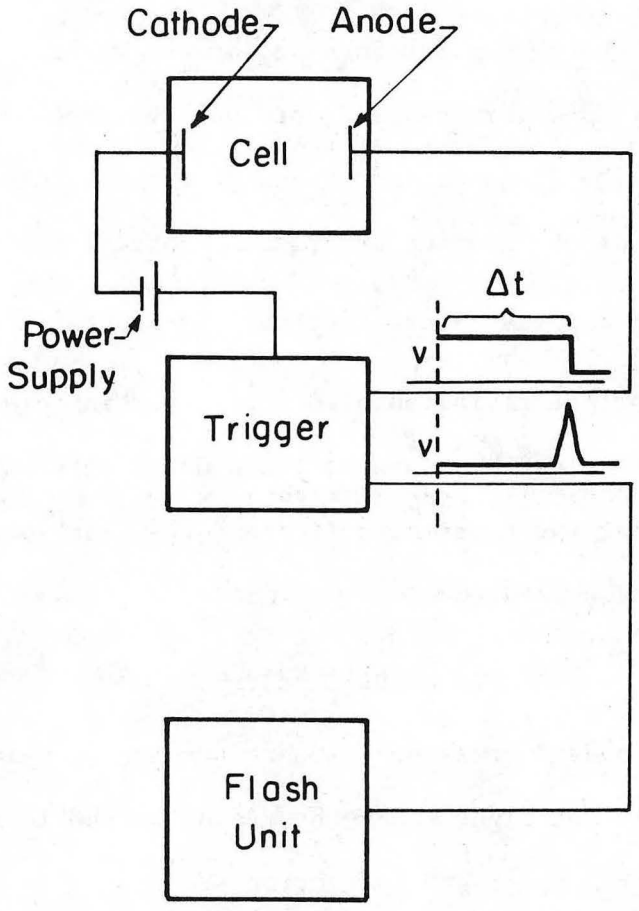

Fig. 4. Flash trigger circuit for incipient bubble growth studies.

to the flash unit after a variable time delay (13-300 msec). With the cell assembled and filled with the desired electrolyte, the electrical connections made, and the optics focussed at the working electrode surface, the camera shutter was held open and the push button depressed. The light time of the flash was short enough for the film to record un-blurred images of the growing and rising bubbles.

D. Steady State Electrolysis Studies

Photographs of the rising bubbles at the working electrode surface during steady state electrolysis were taken using this same apparatus. However, the trigger was short circuited and the flash was triggered with its own manual pushbutton.

E. Bubble Speeds

The rising speeds of the bubbles were determined using the continuous incandescent light source by measuring the length of the tracks resulting from the light reflection spots on the bubbles as they rose during the 1/200 second exposure. Algebraically combining the distance traveled, the microscope magnification, and the shutter speed gave the velocity of the rising bubbles.

F. Freely Rising Bubble Stream

For the study of bubble size distributions in the electrolyte stream well above the electrode surface, the cell shown in Fig. 5 was used. Built of Lucite, the 12×5×4 cm cell block was bored out through opposing walls 3 cm above the bottom to accept the electrodes, which were both identical in construction to the working electrode shown in

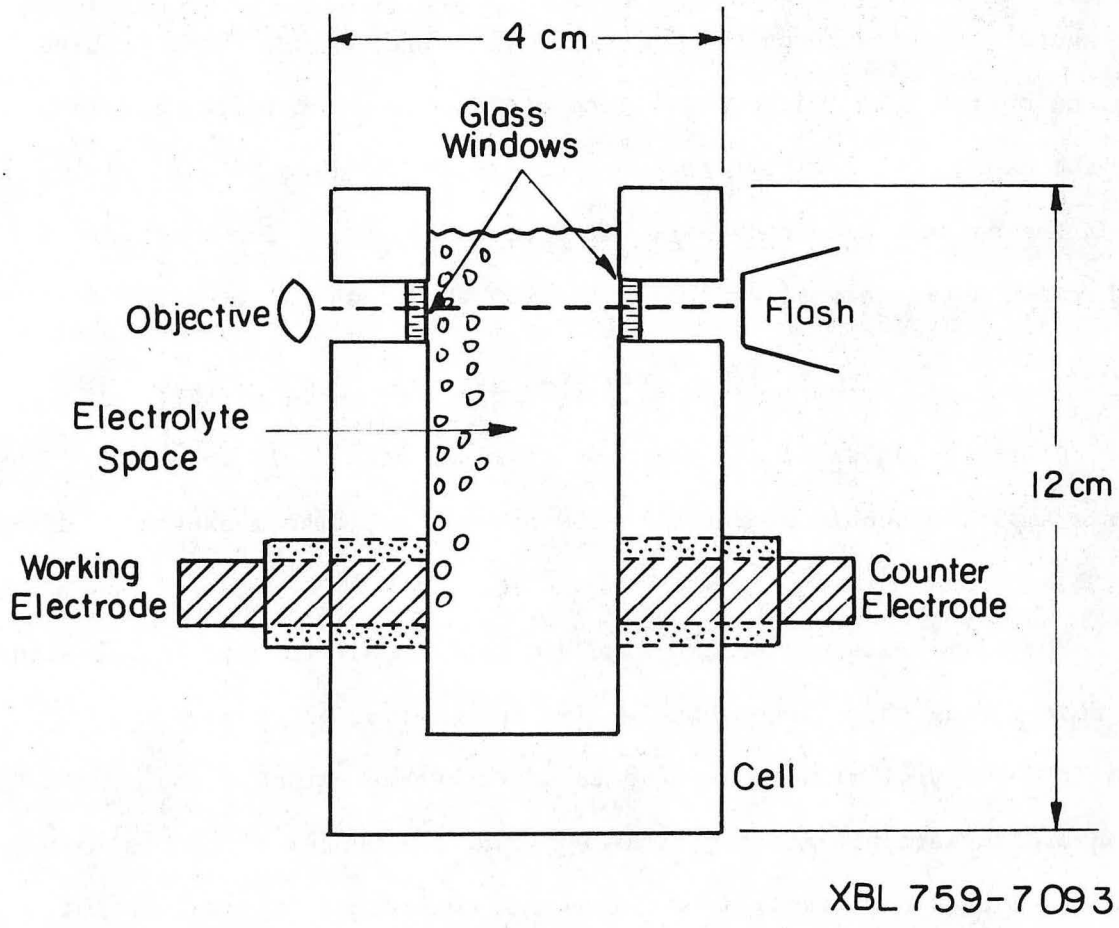

Fig. 5. Free stream bubble size measurement cell construction.

Fig. 2-C. Five centimeters directly above these holes two round pyrex glass windows were installed. Through these the microflash unit, triggered manually, provided back-side lighting of the rising bubbles to the optics. The microscope plane of focus was set in the middle of the bubble stream above the working electrode. The bubbles rising from the counter electrode were far from the plane of focus and did not otherwise noticeably block the light from the flash unit.

G. Data Collection

Distances as small as 5 microns could be accurately measured. Thus, for example, a bubble diameter of 100 microns could be measured to within ±2.5%.

Most all* measured bubble size distributions were normal (Gaussian). In determining the average bubble size for a given electrolysis condition, a preliminary set of data was taken to estimate the sample standard deviation. Based on this estimate the number of bubble diameters that were required to provide a confidence interval of 10% around the true average bubble diameter was calculated for a 95% level of reliability. Thus, with the exception of hydrogen bubble size distributions in sulfuric acid, average bubble diameters reported herein can be considered to be within ±10% of the true average diameter.

---

*The only exceptions being hydrogen bubbles generated in sulfuric acid (see Results).

IV. RESULTS

A. General Observations on Incipient Bubble Growth (See Figures 6-9)

Current densities corresponding to gas evolution rates (G) of 3.5, 7, and 14 $cm^3/cm^2 min$ were studied for the systems H_2/KOH, H_2/H_2SO_4, and O_2/KOH. Very small but distinct bubbles are visible on the electrode surface as early as 13 msec after current initiation. Their sizes are extremely uniform; perhaps 95% are within 5% of the average value. The distribution of nucleation sites is also quite uniform. There are only few bare areas of electrode surface larger in dimension than one or two bubble diameters.

Growth of the bubbles doesn't proceed in such a uniform manner, i.e. some bubbles grow faster than others. The rapid growth sites are evenly distributed among the average and slower growth sites. Eventually the bubbles grow large enough that their diameters approach the center to center bubble separation distance. Once the bubbles touch they coalesce quite rapidly. Despite the fact that rarely have two bubbles been observed in the exact moment of coalescence, such coalescence is evidenced by the decrease in number density of the bubbles and increase in average bubble diameter as time progresses. The coalesced bubbles remain attached to the electrode surface and continue to grow until again they overcome the separation distance between them, when coalescence again takes place. For the first generation of bubbles, since all were nucleated nearly simultaneously, this growth and coalescence process is synchronous over the entire electrode. When

the bubbles on the surface reach a certain average diameter they become permanently disengaged from the electrode surface. The rising sheet of detached bubbles accelerates quite rapidly to a velocity which is approximately the sum of the electrolyte velocity (7-18 cm/sec) and the bubble terminal rise velocity (1-3 cm/sec). The steady state flow field along the small electrode used in this study was observed to be established within a second of commencement of electrolysis. The swift upward flow of gas bubbles and electrolyte past the surface has various effects on the bubbles attached to the surface. For example, in 5M KOH hydrogen bubbles act like billiard balls, in that they generally undergo elastic collisions near the electrode surface. Coalescence between rising bubbles is frequent only in the turbulent stream well above the site of electrolysis. On the other hand, hydrogen bubbles generated from 5M sulfuric acid behave quite differently. During steady state electrolysis the bubbles slide upward while attached to the electrode surface. As they overtake smaller bubbles they absorb or "scavenge" them. Consequently one observes fewer but much larger bubbles on the surface and rising along it.

B. 5M KOH/H_2

1. Incipient Surface Growth

Figures 6 and 7 present a photographic sequence on the incipient surface growth of bubbles. Bubble growth proceeds through the combined mechanisms of individual growth by mass transfer of dissolved gas into bubbles and coalescence of neighboring bubbles when they grow close

enough to touch. Characteristically this happens in such a way that the bubble size distribution at any given instant is very narrow, that is, all the bubbles are of nearly equal size. When coalescence occurs, the newly formed bubble becomes re-attached to the electrode at a point which usually lies on the line between centers of the formerly distinct bubbles. In Fig. 10 the average bubble diameters and number densities are plotted versus time for the gas evolution rates studied. The effect of increasing the gas generation rate is seen to be an increase in the growth rate of the bubbles. As time approaches infinity the bubble diameter curves asymptotically approach 150 microns, which corresponds to the average diameter of the rising bubbles measured during steady state electrolysis. Although the maximum interval was too short to show the complete growth curve at 3.5 $cm^3/cm^2 min$, during steady state electrolysis the rising bubbles were as large as those evolved at higher rates.

At 14 $cm^3/cm^2 min$. the bubbles reach their final size within 130 msec after current initiation, whereas this requires almost 300 msec at 7 $cm^3/cm^2 min$ and well over 300 msec at 3.5 $cm^3/cm^2 min$.

2. Coalescence During Rise

From the photographs of incipient bubble growth it is seen that coalescence is a most common event on the surface of the electrode. Coalescence of bubbles during rise is another matter. This was analyzed by comparing the size distribution of the rising bubbles near the electrode surface to that of the bubble stream a considerable distance (5 cm) above the electrode surface. Figure 11 shows the free stream

bubbles, in which can be seen the noticeably larger ones which were produced through coalescence. Thus considerable coalescence does occur in the rising bubble stream.

C. 5M H_2SO_4/H_2

1. Incipient Surface Growth

Figure 8 shows the incipient bubble growth sequences for these conditions. Hydrogen bubble growth in sulfuric acid is markedly different from that in potassium hydroxide (see Fig. 12). First, the bubble growth rate (for a given gas generation rate) is twice as large in acid, and consequently the number density of bubbles is much smaller. Second, the bubbles growing in acid do not approach any asymptotic size limit with time. What happens is that as they slide upward along the surface the larger bubbles "scavenge" smaller bubbles in their path. These larger bubbles thus grow even more and the smaller bubbles have less of a chance of growing undisturbed to a larger size. As a result, the size distribution has one peak at a very large value (perhaps 700 microns) and another at about 125 microns. Because of this bimodal size distribution it is senseless to speak of an average bubble diameter at which separation occurs. Consequently the plots of bubble diameter vs. time for the incipient growth studies are quite subjective, in that the bubble averages include only those bubbles whose diameters were distributed about the larger average diameter of the bimodal distribution.

D. 5M KOH/O_2

1. Incipient Surface Growth

Figure 9 shows the photographic sequences of incipient growth of oxygen bubbles in 5M KOH. The characteristics of this growth are more similar to hydrogen bubble growth in caustic rather than in acid, primarily because the bubbles sliding upward along the electrode surface do not scavenge the smaller bubbles in their paths as extensively as hydrogen bubbles growing in acid. As a result the bubble size distribution is quite narrow. Figure 13 represents graphically the bubble growth rate and number density variation with time. Several features on these curves are worthy of note. First, the incipient bubble growth curves for 14 and 7 cm^3/cm^2min. approach an asymptotic limit of 250 microns which is distinctly below the measured value of the average rising bubble size during steady state electrolysis. Second, there is remarkable linearity in the bubble growth rate dependence on gas generation rate. In other words, after 50 msec. at 14 cm^3/cm^2min. we obtain the same image as after 100 msec at 7cm^3/cm^2min. In precise terms, the number and sizes of bubbles are identical between one gas generation rate and another when compared at equal numbers of coulombs passed. Figure 14 is a replot of the data in Fig. 13, having an abscissa of coulombs passed instead of time. It is seen that the bubble growth curves thus plotted nearly coincide, at least until such time that bulk bubble separation from the surface has taken place.

The oxygen bubble growth rate in KOH is about 1.5 times higher than the hydrogen growth rate in KOH (Figs. 10 and 13), when compared at equal gas generation rates ($cm^3/cm^2 min$). Also the number density of oxygen bubbles decreases with time much more quickly than that of hydrogen bubbles. These two observations lead to the conclusion that coalescence of bubbles growing on the surface occurs to a much larger degree for oxygen than hydrogen.

E. Electrolyte Velocity

A stream of rising gas bubbles produces an upward flow of electrolyte along with it. Each bubble produces a drag force on the surrounding liquid as it rises at its terminal velocity. The sum of these individual drag forces over all the bubbles in the stream can be quite substantial. At steady state a balance is reached between this and the viscous and inertial forces tending to oppose it, as expressed by the law of conservation of momentum. The resultant upward velocity of the gas-liquid mixture can be substantially greater than the typical free convection velocities found in systems where the density differences are caused by the concentration gradient of dissolved ionic species, such as in metal deposition or dissolution. Table 1 presents the electrolyte velocities determined from observations of bubble velocities near the surface of the electrode employed in this study.

Table 1. Free Convection Electrolyte Velocities

System	G($cm^3/cm^2 min$) 14	7	3.5
H_2/KOH	17cm/sec	15cm/sec	7cm/sec
H_2/H_2SO_4	20	12	8
O_2/KOH	15	16	7
average	17.3	14.3	7.3

The electrolyte velocity V was determined by subtracting the terminal rise velocity V_∞ of the bubbles[20] from the optically determined average bubble velocity V_o (see EXPERIMENTAL). A second order correction for void fraction has been presented by Rousar,[21] but it was not used here because the void fraction was unknown and because the magnitude of the correction is smaller than the experimental uncertainty. Two points must be made concerning the velocities in this table.

1. The velocities measured for all three systems at a given gas generation rate ($cm^3/cm^2 min$) are within 20% of each other, the limit of experimental precision. Thus, to a first approximation, the velocity can be considered to be a function only of gas generation rate. Differences in bubble growth characteristics from one system to the next introduce only second order differences in the velocity fields adjacent to the electrode surface.

2. The electrolyte velocity must vary with normal distance from the electrode surface, reaching a maximum somewhere in the middle of the rising bubble-electrolyte stream. Since speeds of bubbles which were rising at various distances from the electrode surface were used to obtain the average bubble speed, the electrolyte velocity calculated from this average bubble speed is thus an average over the electrolyte velocity field.

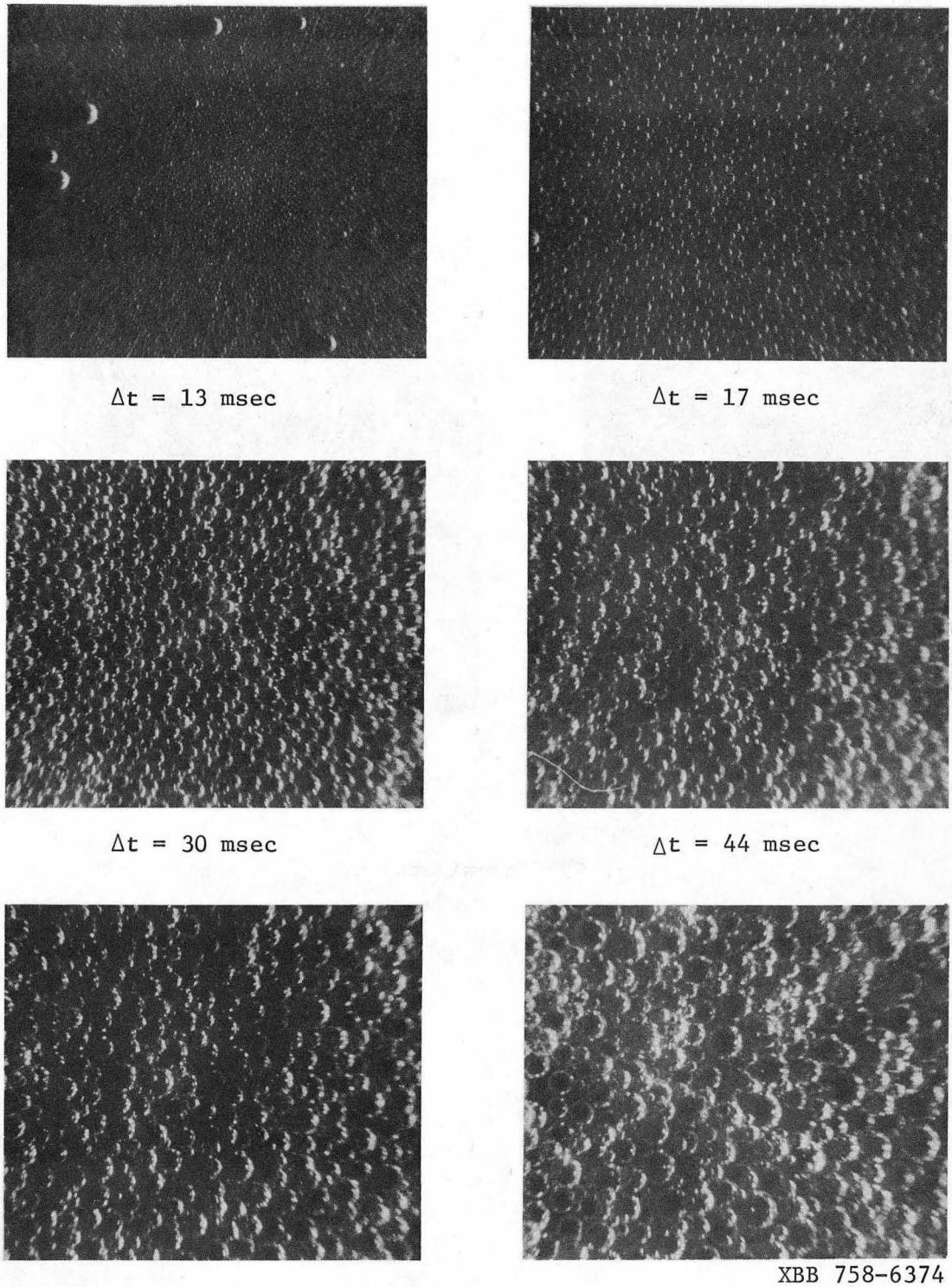

Fig. 6. Incipient bubble growth photographic sequence: hydrogen bubbles in 5M KOH electrolyte, 14 cm^3/cm^2 min (magnification 45×)

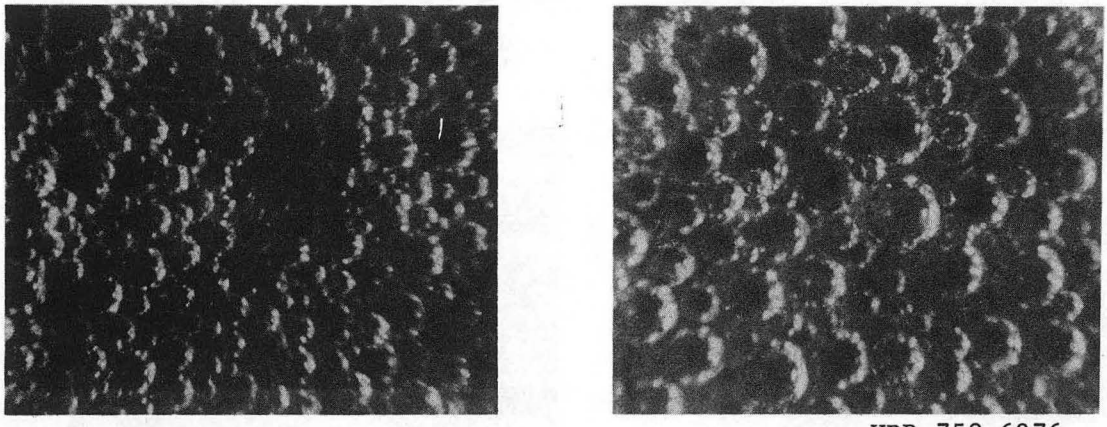

XBB 758-6376

Δt = 89 msec

Δt = 130 msec

Fig. 6. (continued)

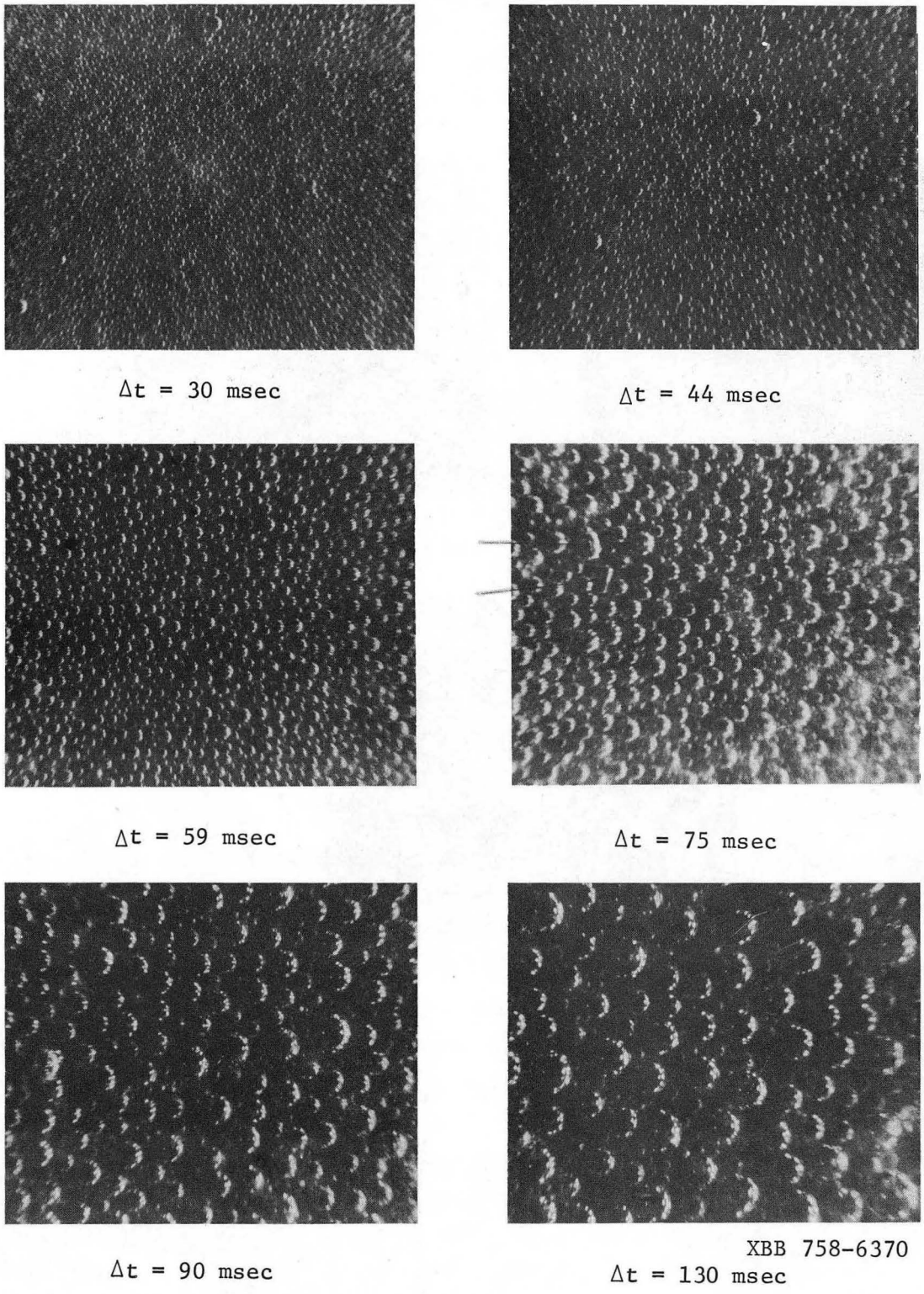

Fig. 7. Incipient bubble growth photographic sequence: hydrogen bubbles in 5M KOH electrolyte, 7 cm^3/cm^2 min. (magnification 45×) (arrows point to coalescing bubbles)

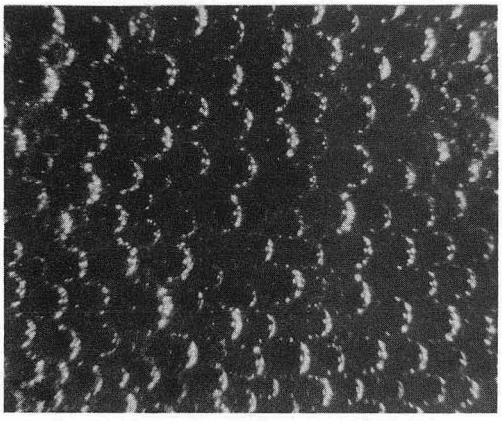

Δt = 180 msec

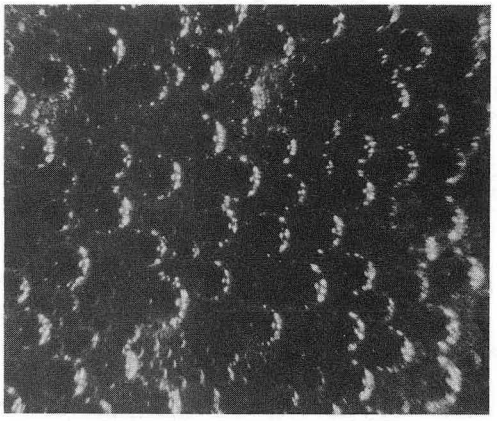

Δt = 240 msec

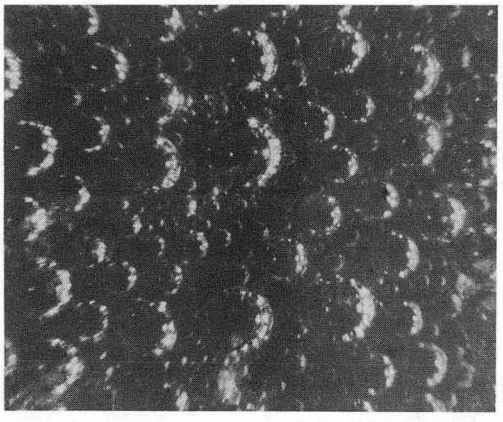

XBB 758-6375

Δt = 290 msec

Fig. 7. (continued)

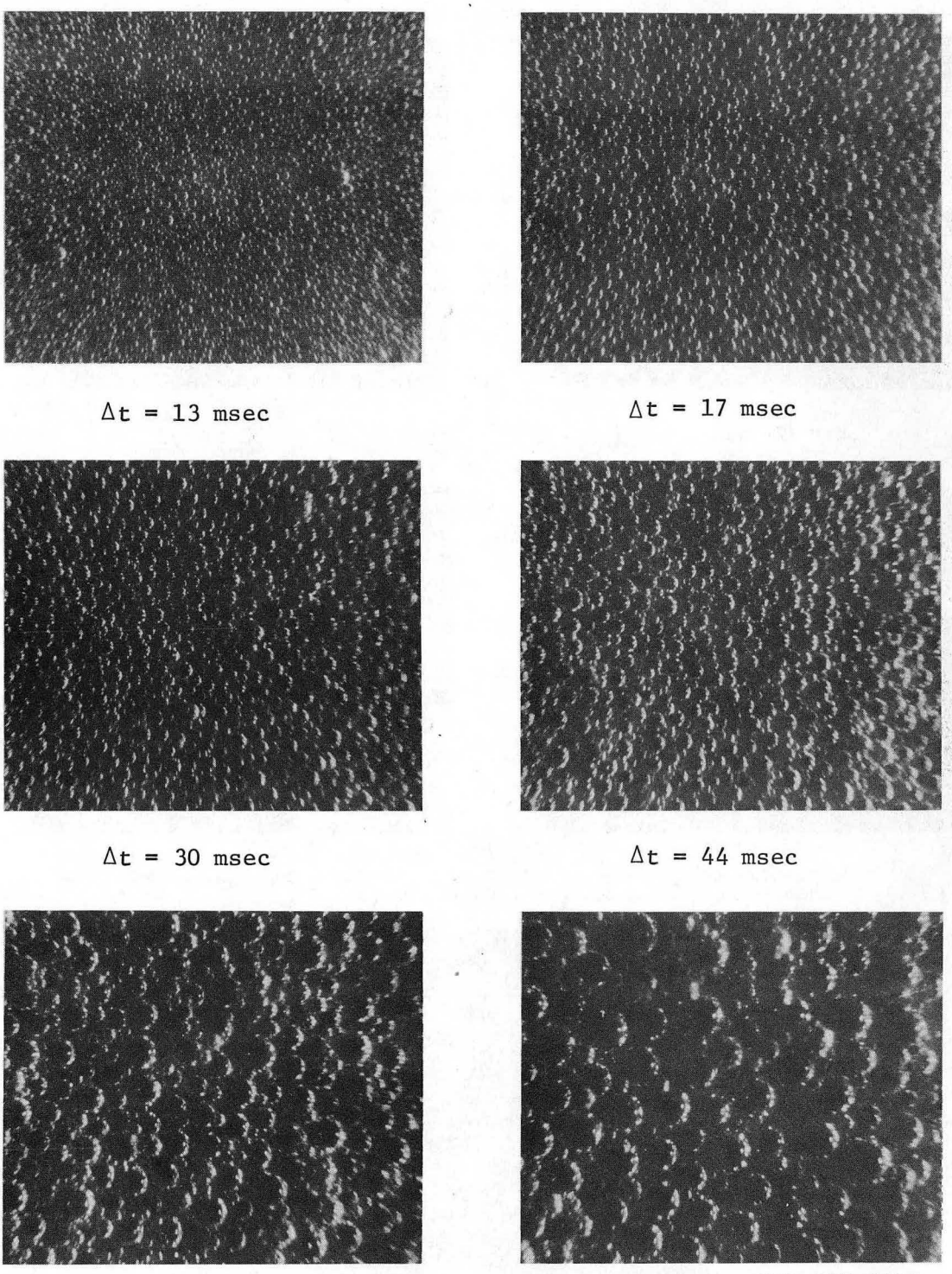

Fig. 8. Incipient bubble growth photographic sequence: hydrogen bubbles in 5M H_2SO_4 electrolyte, 14 cm^3/cm^2 min (magnification 45×) (arrows point to coalescing bubbles)

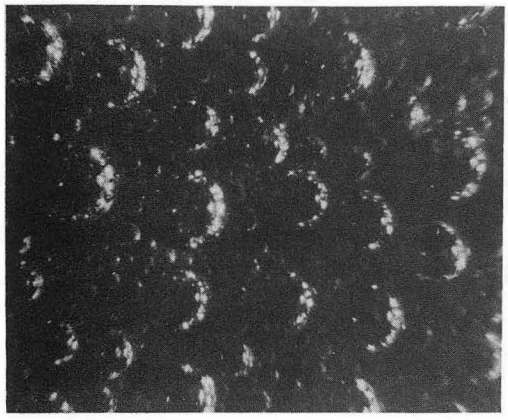

Δt = 89 msec

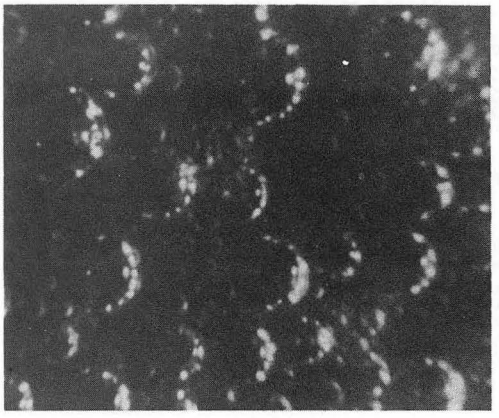

Δt = 130 msec

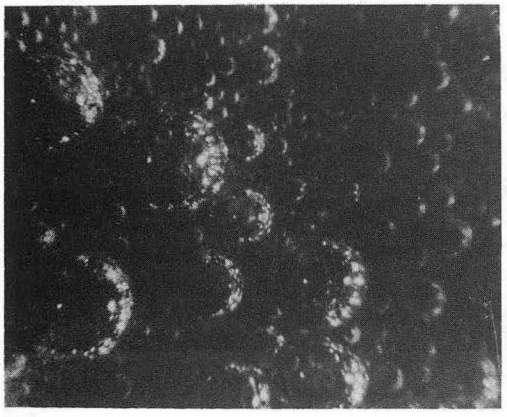

Δt = 180 msec

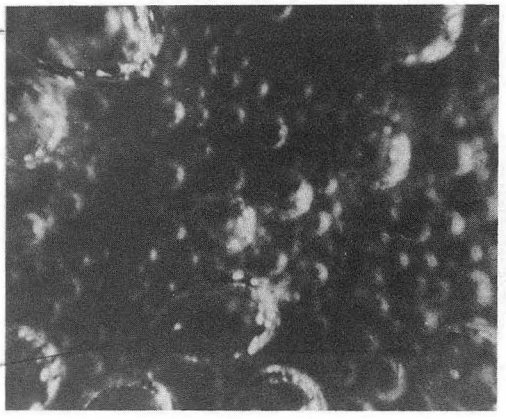

Δt = 240 msec

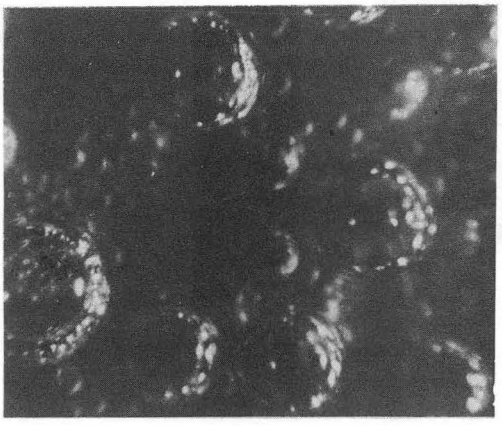

XBB 758-6369

Δt = 290 msec

Fig. 8. (continued)

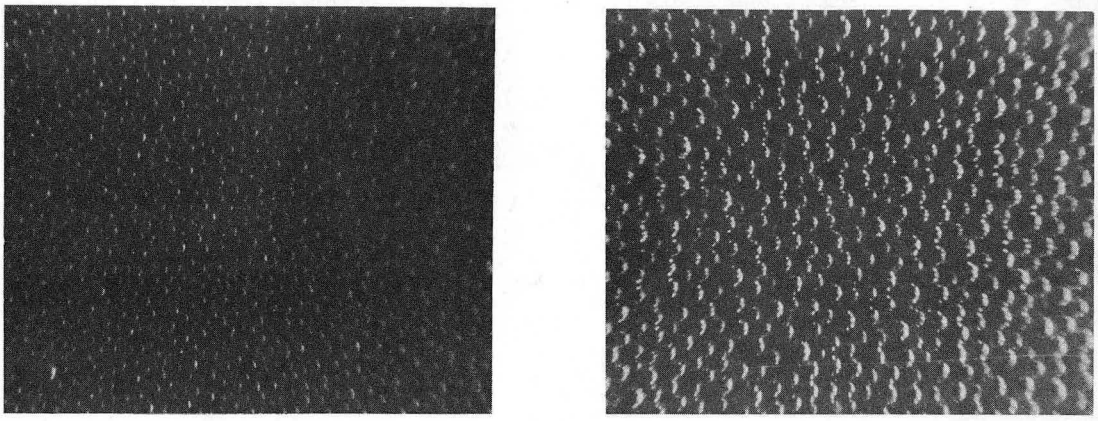

Δt = 13 msec

Δt = 17 msec

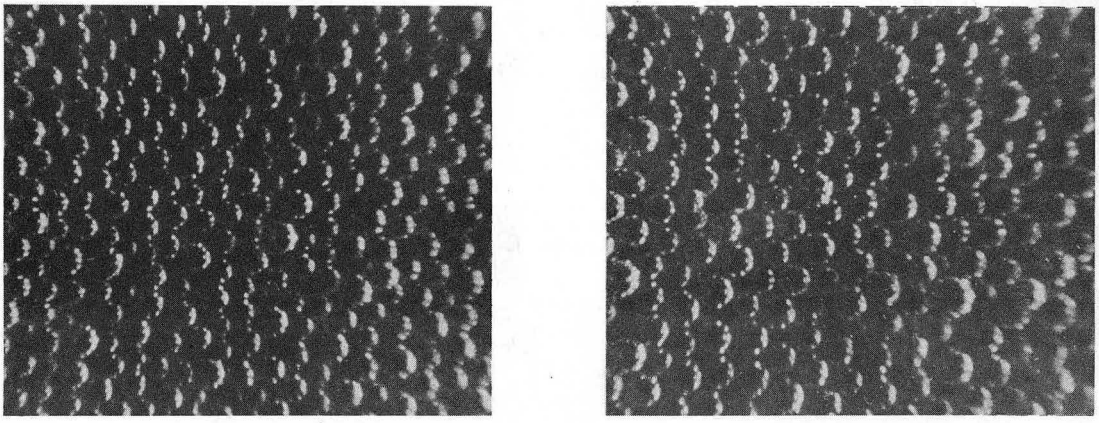

Δt = 30 msec

Δt = 44 msec

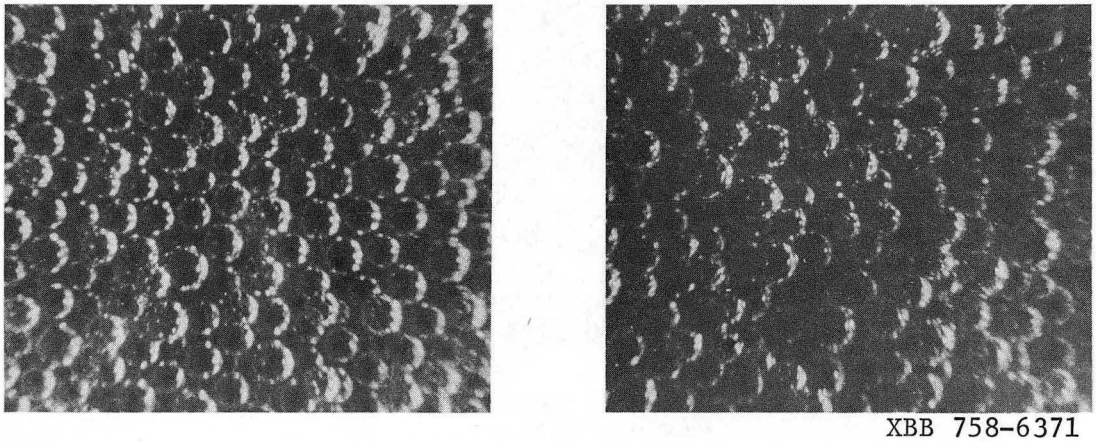

XBB 758-6371

Δt = 59 msec

Δt = 75 msec

Fig. 9. Incipient bubble growth photographic sequence: oxygen bubbles in 5M KOH electrolyte, 14 cm^3/cm^2 min (magnification 45×)

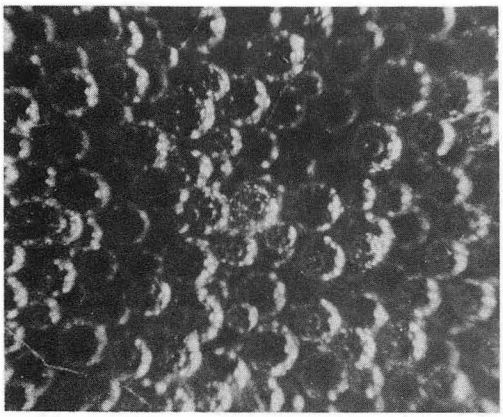

Δt = 89 msec

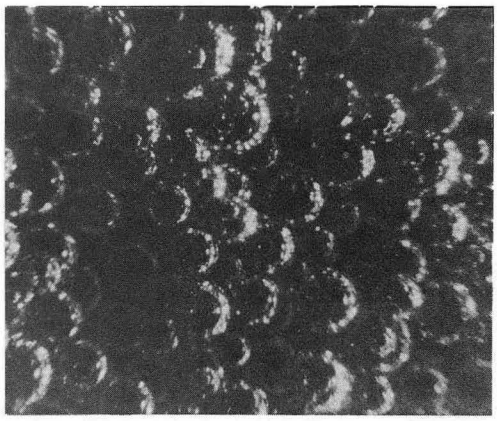

Δt = 130 msec

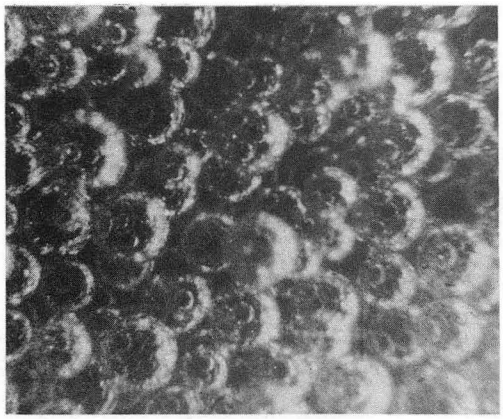

Δt = 30 msec

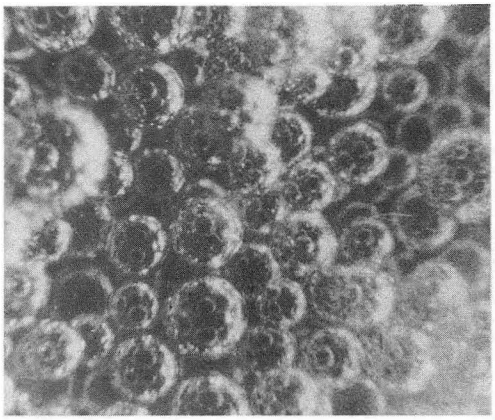

Δt = 44 msec

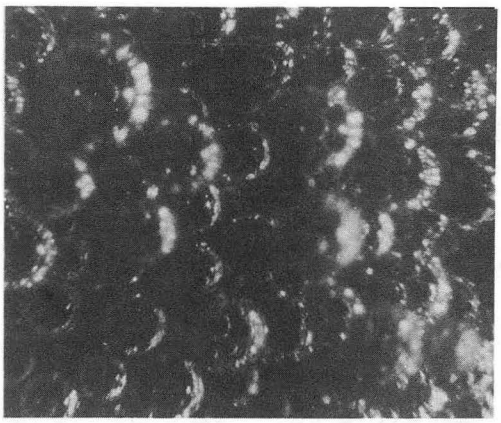

XBB 758-6372

Δt = 290 msec

Fig. 9. (continued)

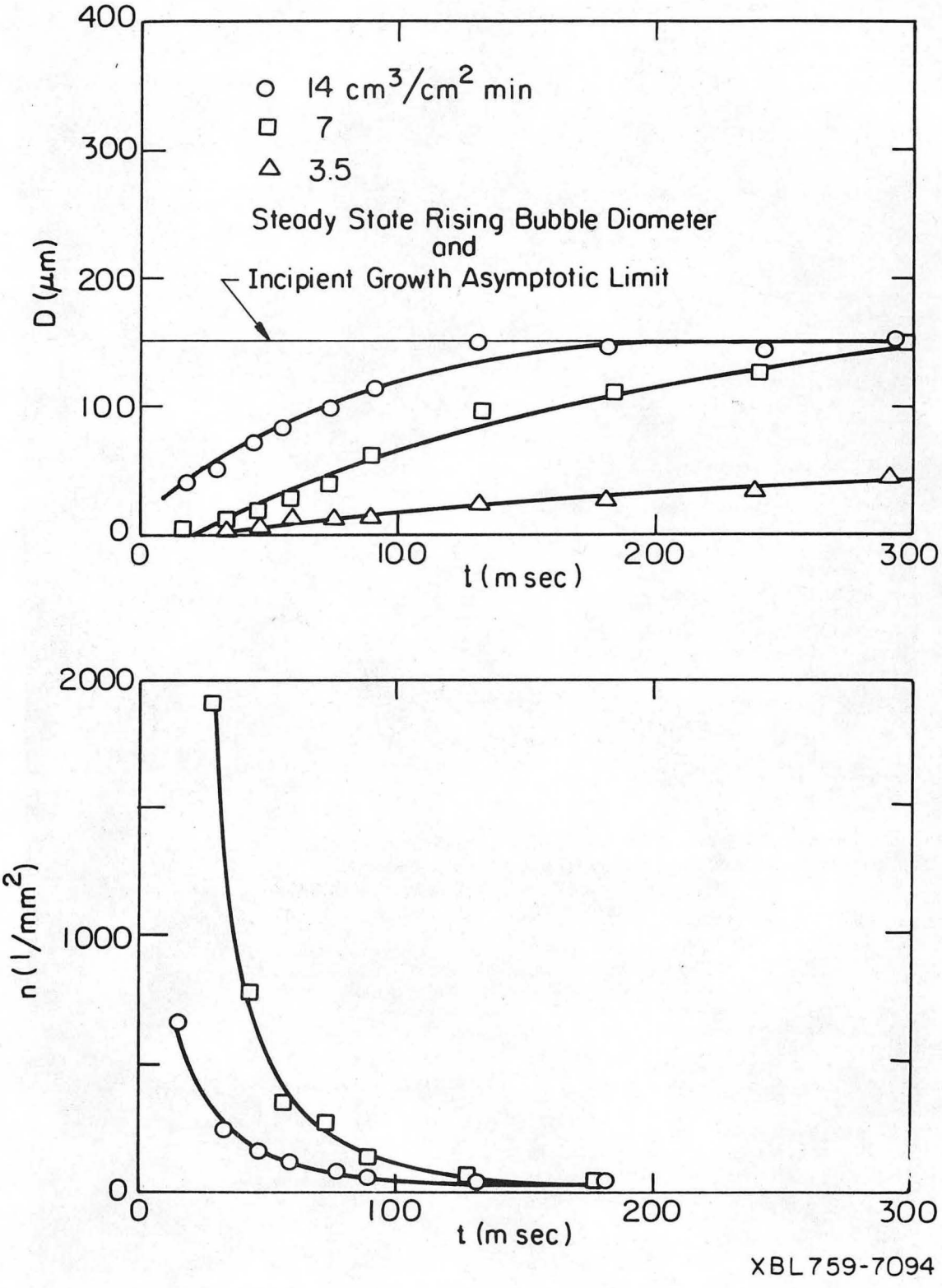

Fig. 10. Incipient bubble growth average bubble diameter and number density curves: hydrogen bubbles in 5 M KOH electrolyte.

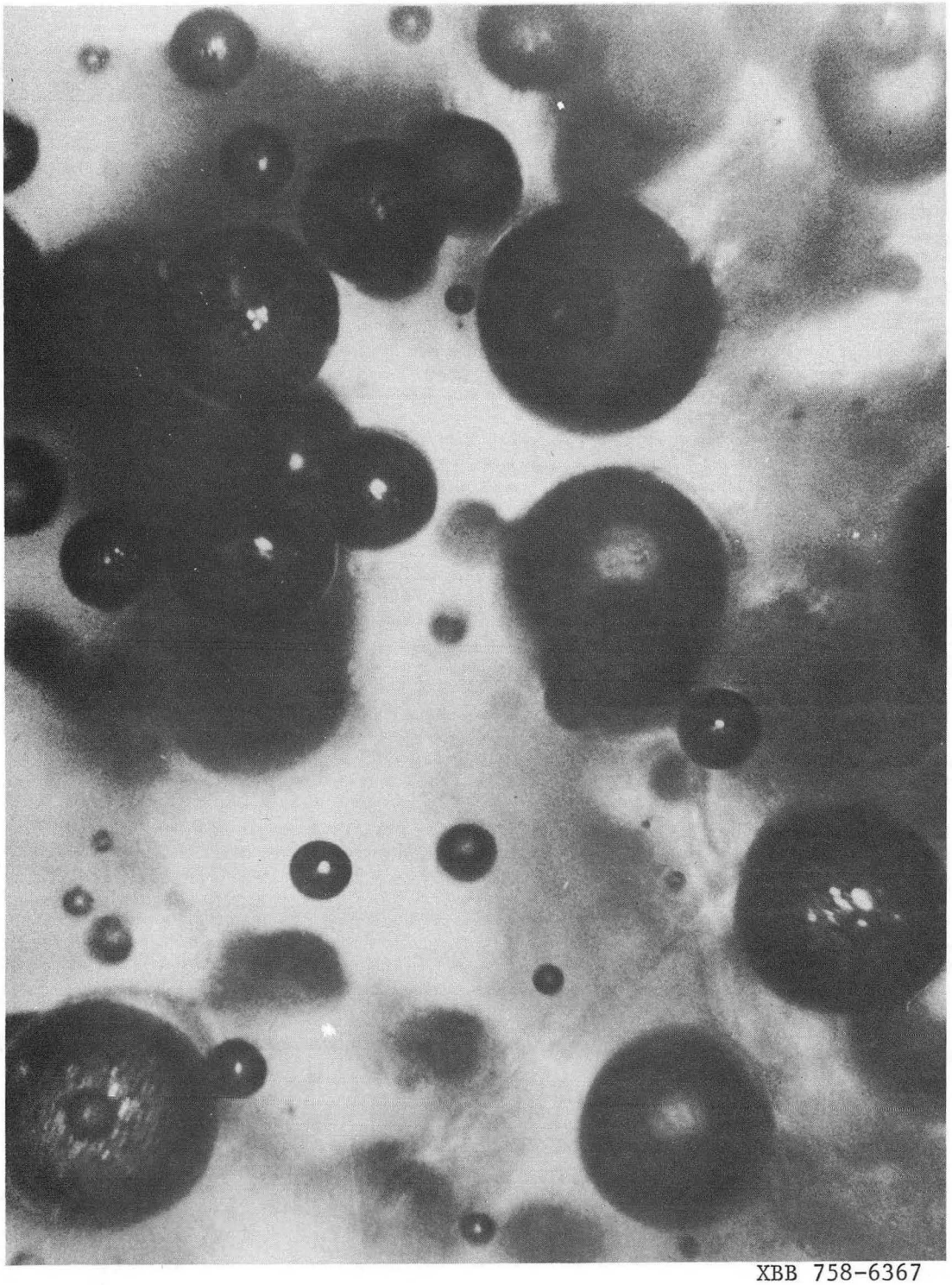

XBB 758-6367

Fig. 11. Free stream bubbles: hydrogen bubbles in 5M KOH electrolyte, 14 cm^3/cm^2 min. (magnification 130×)

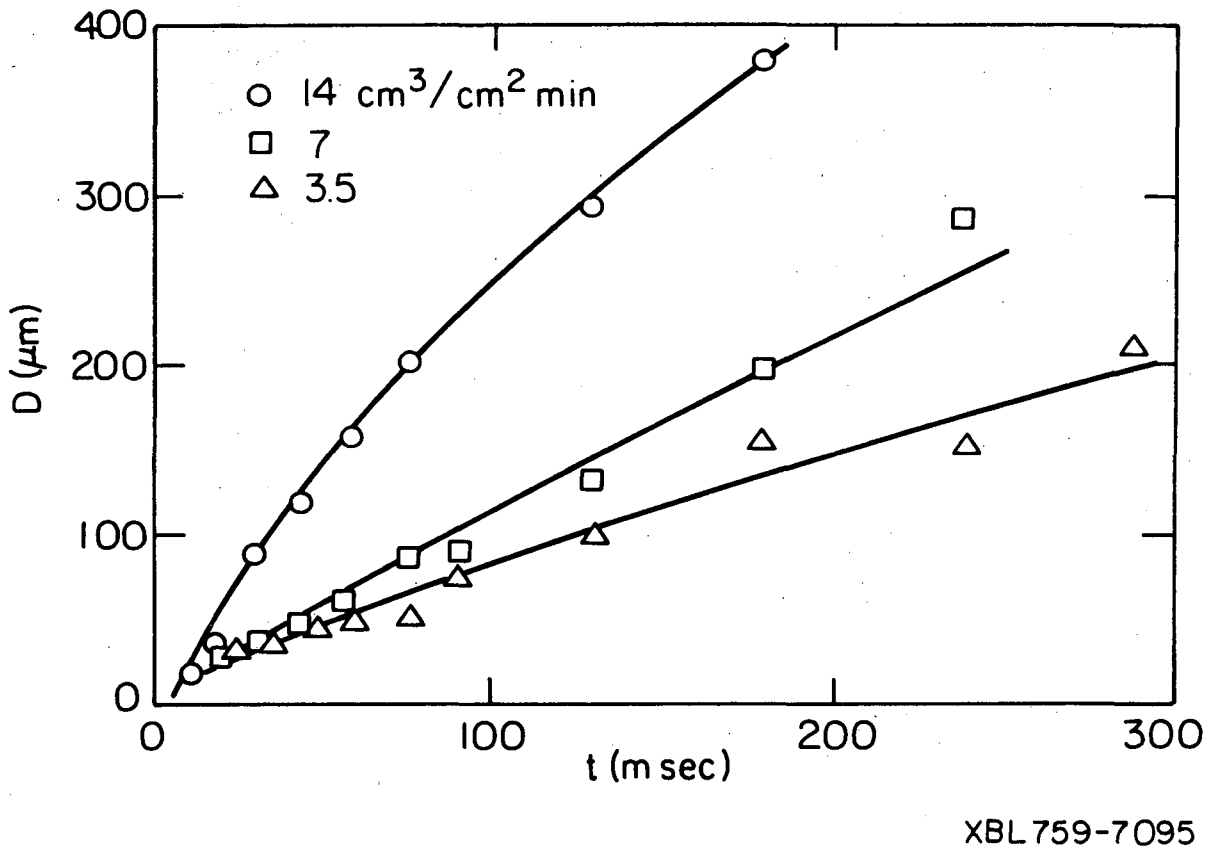

Fig. 12. Incipient bubble growth average bubble diameter curves: hydrogen bubbles in 5M H_2SO_4 electrolyte.

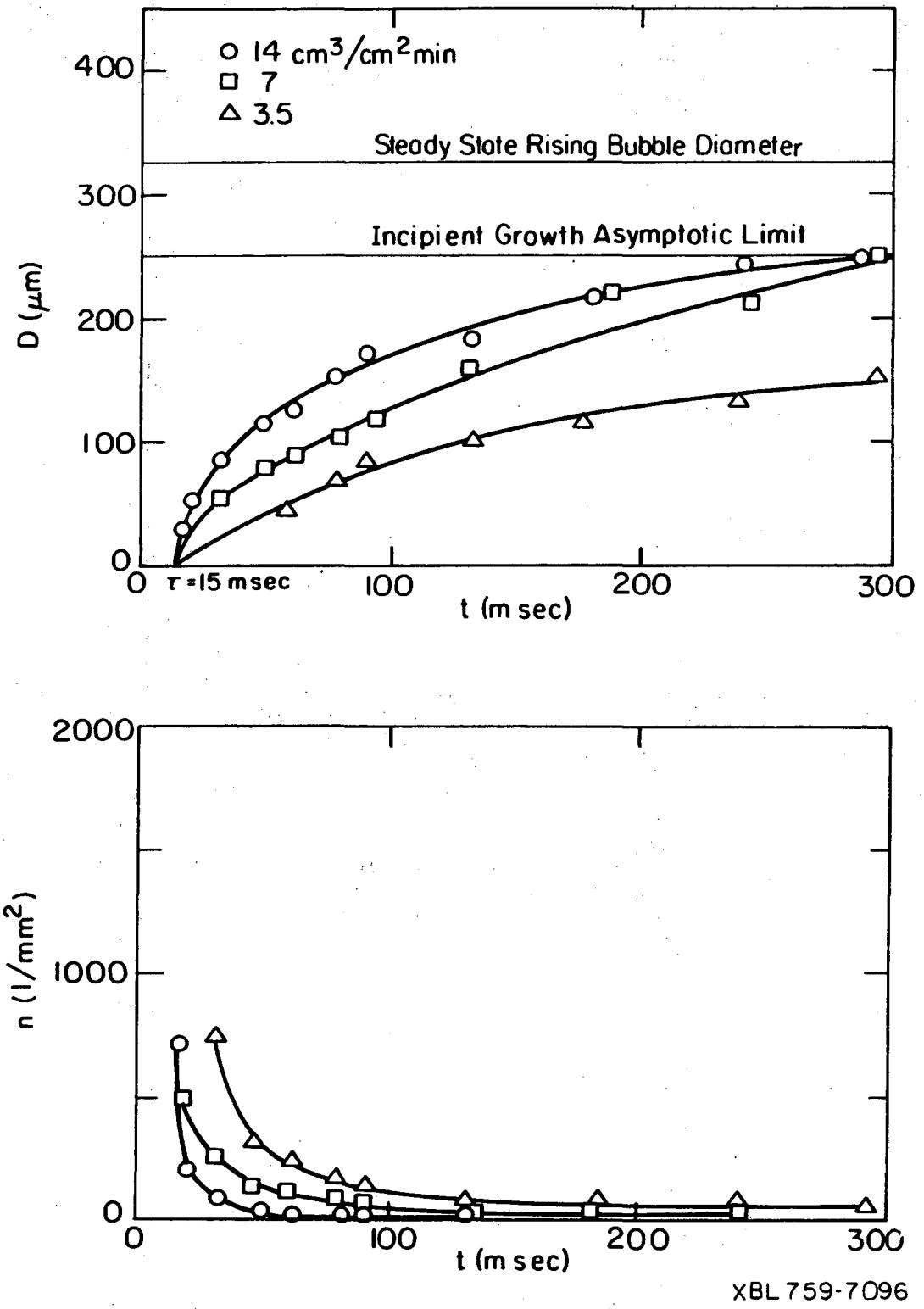

Fig. 13. Incipient bubble growth average bubble diameter and number density curves: oxygen bubbles in 5 M KOH electrolyte.

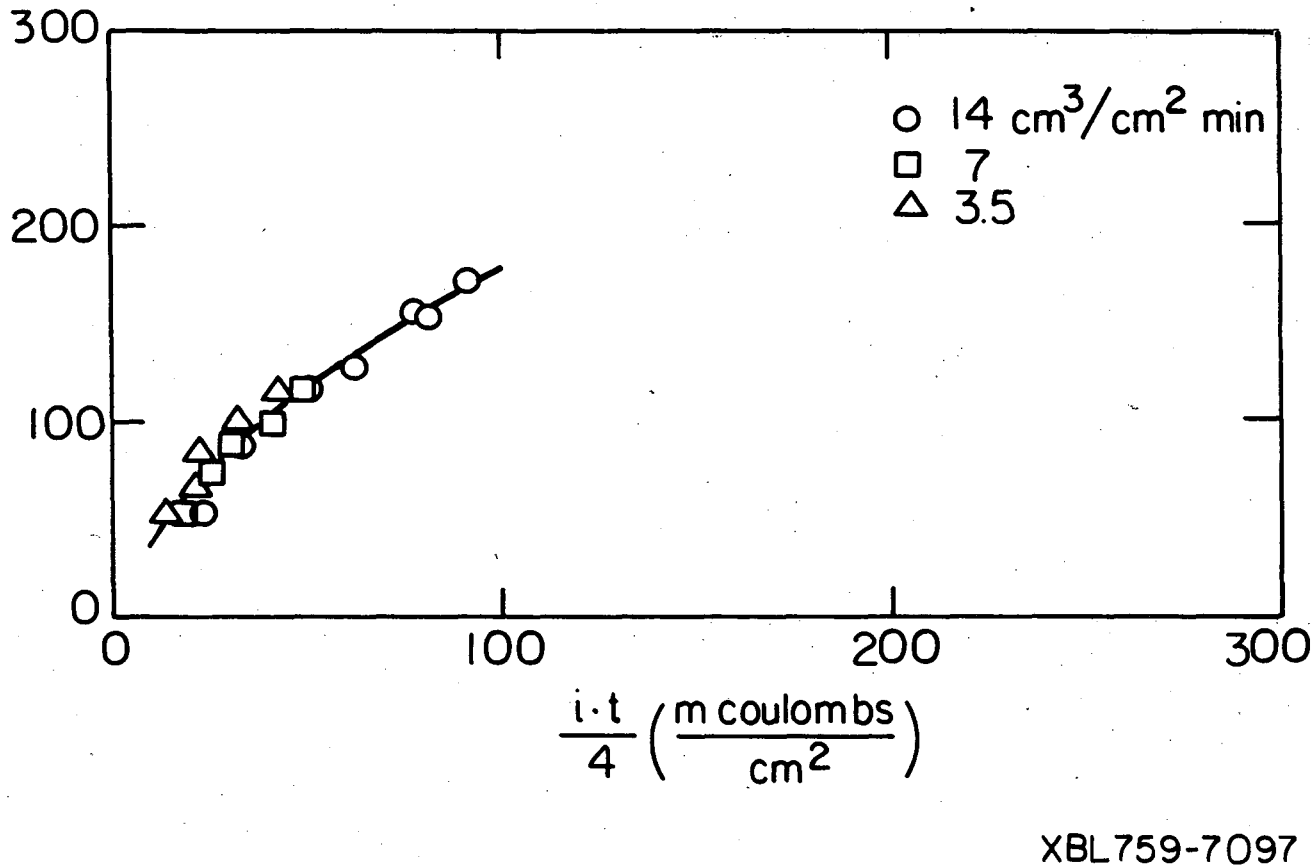

Fig. 14. Replot of incipient bubble growth bubble diameter curves on an abscissa of coulombs passed: oxygen bubbles in 5 M KOH electrolyte.

V. DISCUSSION

A. Nucleation and Bubble Growth

The number density of bubbles growing on the surface of an electrode is determined by the bubble size distribution. That is, neighboring bubbles are initially separated by a finite distance but quickly grow large enough to touch and coalesce. As a result, fewer bubbles having correspondingly larger volumes are formed. These larger bubbles will continue to grow until they touch and coalesce with one or more of their neighbors. As time progresses the coalescence phenomena meld and the bubble distribution on the surface is close-packed.

In comparing growth characteristics in KOH and H_2SO_4, the degree of coalescence of large bubbles with smaller bubbles as the former slide upward along the surface sets gas generation in sulfuric acid apart from that in KOH. This large degree of coalescence in acid has been previously observed by Venczel.[17] It can be attributed to the difference in wettability of the electrode surface between sulfuric acid and potassium hydroxide.

The effect of electrode potential on interfacial tension is easily seen by comparing the maximum bubble diameters reached in the incipient growth studies between hydrogen and oxygen evolution in KOH. That approximately the same electrolyte concentration exists at both electrode surfaces can be proven by the following calculation. Ibl and Venczel[16] measured an effective Nernst boundary layer thickness δ_N = 5 microns at a hydrogen evolving electrode for a gas evolution rate of 14 $cm^3/cm^2 min$.

For an approximate diffusivity of $D=3\times10^{-5}$ cm^2/sec[22] for KOH in water, the concentration change at the cathode surface can be estimated* from

$$\Delta C \approx \frac{\delta_N}{D} \times \frac{i}{nF} \quad .$$

A gas generation rate of 14 $cm^3/cm^2 min$ corresponds to a current density of 2 a/cm^2 for hydrogen evolution. The value of ΔC thus calculated is 3.5×10^{-4} $moles/cm^3$. For a bulk KOH concentration of 5M this difference is negligible. Similar results would be obtained for the magnitude of the concentration difference at the anode. Approximate electrode potentials were measured, during hydrogen and oxygen evolution, against a reference hydrogen electrode which was connected to the cell via a backside capillary. The IR voltage drop included in these measurements was estimated to be about .1v.[23] These potentials were converted to potentials relative to a normal calomel electrode and are shown in Table 2. By locating these potentials on the electrocapillary curve for KOH[24] one finds the interfacial tension to be 300±20 dynes/cm for hydrogen evolution and 400±20 dynes/cm for oxygen evolution. Since the value for oxygen evolution is 1.3 times greater, the adhesive force of the bubbles on the surface is also greater and consequently bubbles are expected to separate at larger diameters there.

*This neglects migration of OH^- ions and the loss of water molecules at the cathode, which have opposing effects on the OH^- concentration there. However this is only an order-of-magnitude calculation.

Table 2. Electrode Potentials for Gas Evolution Relative to the Normal Calomel Electrode.

$G(cm^3/cm^2min)$	H_2/KOH	O_2/KOH
3.5	-1.55 volts	+.39 volts
7	-1.58	+.42
14	-1.64	+.46

all values are ± .1 volt

These results are in accordance with the findings of Kabanov and Frumkin.[2]

Another difference between hydrogen and oxygen evolution in caustic is that the latter exhibits a certain degree of the "scavenging" effect. That is, the oxygen bubbles, while sliding upward along the surface, absorb smaller bubbles in their paths.* This is reflected in the disparity between the incipient growth curve asymptotic bubble diameter limit and the steady state diameter of the rising bubbles (Fig. 13). Due to the in-phase growth of the first generation of bubbles during incipient growth the sliding bubbles are not as likely to encounter smaller bubbles in their paths. Thus when they finally leave the surface they lack the volume contributed by scavenged bubbles,

*but not to the extent of that observed by hydrogen bubbles in H_2SO_4. The size distributions of oxygen bubbles in KOH remained Gaussian.[4]

whereas during steady state electrolysis that volume is present. For hydrogen evolution in KOH (Fig. 10) the incipient growth maximum and steady state rising bubble diameter are equal, showing that the scavenging effect is not prominent there.

B. Comparison of Calculated and Measured Gas Generation Rates

At a given current density (assuming 100% current efficiency) the calculated rate of gas generation G is given by Faraday's Law;

$$G = \frac{i}{nF} \cdot \bar{V}$$

where n is the number of gram-equivalents per mole, F is Faraday's Constant, i is the current density, and $\bar{V}$ is the molar volume of the gas. After a time period t of gas evolution the calculated volume of gas evolved per unit area of electrode surface is

$$\nu_c = G \cdot t \ .$$

For incipient bubble growth the measured volume of gas generated per unit area of electrode surface is

$$\nu_m = n_b \cdot V_b$$

where n_b is the number density of bubbles and V_b is the average bubble volume.

Figure 15 is a plot of the measured gas volume (normalized to a scale of 0-1 by dividing by the calculated gas volume) versus time for hydrogen evolution in KOH. The disparity between calculated and measured gas generation rates can be partly attributed to the establishment of the highly gas-supersaturated liquid layer near the electrode

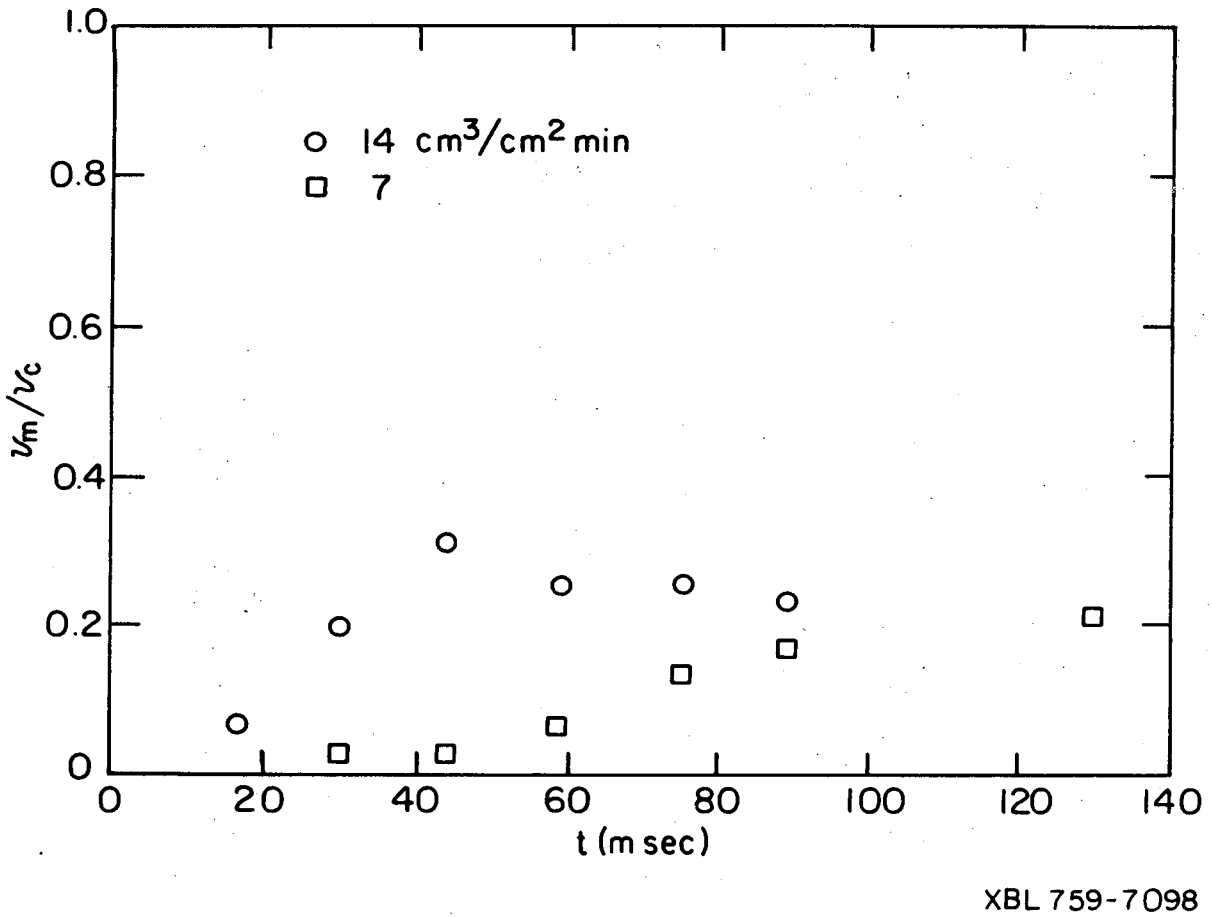

Fig. 15. The ratio measured gas volume/calculated gas volume versus time: hydrogen generation in 5 M KOH electrolyte.

surface, as measured by Bon.[13] However, this cannot be the full explanation, as the following calculation shows: Cheh[1] presents the solution of the one-dimensional diffusion equation describing the dissolved gas concentration immediately after commencement of electrolysis at constant current as

$$C = C_\infty + q\sqrt{\frac{4t}{D}}\ \text{ierfc}\ \frac{x}{2\sqrt{Dt}}\ ,$$

where ierfcz is the integrated error function

$$\text{ierfcz} = \frac{2}{\sqrt{\pi}}\int_z^\infty (t-z)e^{-t^2}\,dt\ ,$$

C_∞ is the bulk concentration, t is the time after commencement of electrolysis, D is the dissolved gas diffusion coefficient, x is the perpendicular distance from the electrode surface, and q is the rate of gas evolution (moles/cm^2sec). This can be applied as an approximation to the present situation by using a value of q that represents the amount of gas generated which is not observed in the growing bubbles. Thus in Fig. 15 it is seen that about 20% of the calculated rate of gas generation is seen in the growing bubbles, leaving 80% of the gas in the diffusion process. Plugging in the value of gas generation rate corresponding to 2 a/cm^2 for hydrogen evolution, multiplied by 0.8, and the values

$$C_\infty = 0\ \text{gm/cm}^3$$
$$D = 1.55\times10^{-5}\ \text{cm}^2/\text{sec}^{25}\ ,$$

the dissolved gas concentration at the electrode surface (x=0) after 100 msec. is calculated to be $\sim 12.8\times10^{-4}$ moles/cm^3. This corresponds (using a hydrogen solubility of 0.078×10^{-3} moles/l.atm. in KOH[25]) to an excess hydrogen pressure of 1600 atm. A crude extrapolation of Bon's data to this current density gives a value of 1000 atm, which, when one considers that his experiments were conducted in sulfuric acid (in which different transport properties and solubilities exist) is consistent with this result. Therefore the buildup of the highly supersaturated region at the electrode surface may well account for the differences observed between calculated and measured gas volumes present in the incipient electrolysis studies.

C. Comparison of the Forces Acting on a Gas Bubble Attached to a Vertical Electrode Surface

To this day an exact description of the force which holds a gas bubble onto a vertical surface is not available. Even more mysterious is what determines the separation diameter of gas bubbles during electrolysis at a finite rate, since in that case, due to the dynamics of the situation, not all the forces acting on the bubbles are at their equilibrium values (specifically the surface forces). To gain some insight, the magnitudes of the forces at play were evaluated for hydrogen bubbles in 5M KOH at the bubble sizes observed. The buoyancy force on a gas bubble is given by

$$B = \frac{\pi}{6} D^3(\rho_L-\rho_g)g$$

where D is the bubble diameter, ρ_L the liquid density, ρ_g the gas density, and g the acceleration due to gravity. For a 150 micron hydrogen bubble in 5M KOH the buoyancy force is 0.22×10^{-2} dynes.

2. Ibl[18] cites a formula for the maximum volume an attached bubble may attain;*

$$V_{max} = (\frac{3}{\pi})^3 \left(\frac{\gamma_1}{\rho_L \cdot g}\right)^{3/2} \theta^3$$

where γ_1 is the gas-liquid surface tension and θ is the contact angle of the bubble on the surface of the electrode. For a 5M KOH solution and a reasonable estimation of contact angle of 12°, based on visual observations, the maximum bubble diameter was calculated to be 700 microns. This represents the balance of the buoyancy and adhesive forces.

The maximum observed diameter is about 5 times smaller than that calculated by Ibl's formula. Also, in incipient bubble growth no velocity profile exists to cause a form drag on the bubbles. Thus one is left to question what determines the terminal bubble separation diameter. Some insight could be gained by measuring the terminal bubble diameter on the electrode surface at various temperatures, since liquid viscosity, surface tension, and density all vary strongly with temperature. It was found that for hydrogen generation in 5M KOH at 14 $cm^3/cm^2 min$. the exact same bubble growth rates and terminal bubble diameter existed over the temperature range 20-85C. This can only mean that in the separation of the bubbles dynamic, rather than equilibrium,

*This applies only to a horizontal electrode facing up, however, there was found to be no difference in the size distributions of bubbles generated from horizontal and vertical electrodes.

phenomena dominate.

Gas bubbles growing on the electrode surface undergo multiple coalescence with their neighbors. These coalescences are very rapid, occurring in 1/2000 sec or less, as shown by Westerheide and Westwater.[8] These authors also showed that when two bubbles coalesce the product bubble is initially separated from the electrode and subsequently returns. The reason for the bubble returning to the electrode is not completely understood.

If the adhesive surface force is large enough, the separation distance between bubble and electrode can be overcome and the bubble will become attached to the surface and continue to grow. However, when one considers the extreme rapidity and violent nature of coalescence it becomes obvious that large inertial forces and high rates of shear are experienced by the surrounding liquid. Eventually the size of product bubble is reached such that the ensuing liquid disturbance manifests a resultant force on the bubble which is greater than the adhesive surface force and the bubble is torn away from the electrode surface. "Bubble separation" is thus not a single event in the lifetime of a bubble, it occurs at each coalescence.

The bubble continues to grow after the final separation, since it is still in the region of supersaturation of dissolved gas. The extent of the growth is determined by its residence time in this region, which is a function of bubble speed and trajectory. Although no exact measurements were made of how much a bubble grows after separation, observations indicate that such growth is minimal. Apparently the

bubble trajectory quickly carries it away from the region of high supersaturation.

D. Extension to Steady State Electrolysis

The bubble growth characteristics observed in the incipient electrolysis studies are not identical to the events occurring on the surface during steady state. In incipient growth all bubbles are nucleated at about the same time shortly after commencement of electrolysis, and their growth is synchronous. However, after the first few generations of bubbles leave the surface, the small differences in growth rates and the effects of the natural convection velocity generated by the rising bubbles cause a randomization of bubble growth, so that at a given instant on the electrode surface one bubble will be just newly formed while its neighbor may be at its separation diameter. Thus the average diameter of the bubbles sitting on the surface will be some value between the two extremes. Likewise the bubble number density will represent a compromise of the out-of-phase bubble growth and the tendency toward close packing. No simple formulas can be applied to the data at hand to extract steady state values for these. A direct measurement technique similar to Venczel's[17] would be the best source of such information.

E. Miscellaneous

As previously mentioned, oxygen bubbles in potassium hydroxide and hydrogen bubbles in sulfuric acid absorb stationary bubbles sitting on the surface as they rise, the latter to a much greater extent than the former. However, no such coalescence occurred at the electrode surface for rising hydrogen bubbles in caustic. Janssen and Hoogland[15] obtained similar results at much lower current densities (30-500 ma/cm^2). The coalescence observed in the free bubble stream well above the electrode surface for this system at first hand may seem inconsistent. A satisfactory explanation may be given as follows: the hydrogen bubbles generated in KOH are smaller than those in H_2SO_4 or oxygen bubbles in KOH. The smaller bubbles are less penetrable and the collisions occurring between rising bubbles near the electrode surface are of insufficient impulse for coalescence to occur; the bubble-electrolyte flow there is uniform and directly upward. However, as the gas-liquid mixture rises the flow becomes more turbulent; eddies are clearly visible. In this region there is more likelihood that bubbles will collide with sufficient impact to overcome the surface forces and coalesce.

Since preferential bubble nucleation sites are generally considered to be at pits or scratches in the electrode metal surface,[5] the effect of surface morphology on bubble nucleation was also studied. Identical incipient bubble growth experiments were carried out on a rough nickel surface (polished with 1/0 grit emery cloth, which leaves a visibly scratched surface) and a smooth one (polished with .05 micron aluminum

oxide powder, such that a mirror smooth surface results) for all three systems. Surprisingly, identical bubble growth characteristics were obtained on both surfaces. The same bubble growth rate and number density curves were recorded, the maximum bubble diameters remained unchanged, and in all other respects the results were similar on both surfaces. Two conclusions may be drawn from this. First, at these current densities even the slightest surface imperfections (at least as small as .05 microns) are active nucleation sites. Second, the adhesion of bubbles to the surface in the dynamic situation has little to do with its roughness.

Interesting side observations were made after stopping the electrolysis current. Hydrogen bubbles in KOH as large as 70 microns would occasionally remain on the rough surface. However on the very smooth surface only very small bubbles (< 10 microns) would do so. In sulfuric acid bubbles of most any size would remain (some as large as 700 microns) regardless of the surface condition.

As water electrolysis is frequently carried out at much lower current densities than employed here, a separate study was conducted on hydrogen generation in KOH in a lower current density range, extending down to 15 ma/cm^2. It was found that a markedly different regime of electrolysis exists at a current density below 500 ma/cm^2, in that above this the diameter of the rising bubbles during steady state electrolysis is independent of current density, while below 500 ma/cm^2 this is not the case. In fact, as the current density is decreased the average steady state rising bubble diameter also decreases, as does the free

convection velocity. Table 4 presents the experimental results.

Table 4. Average Rising Bubble Diameter and Electrolyte Velocity for Hydrogen Generation in 5M KOH.

$i(ma/cm^2)$	$\bar{D}$(microns)	V(cm/sec)
2000	150	17.3
1000	150	14.3
500	150	7.3
250	122	5.0
122	97	3.4
62	71	1.8
30	64	1.2
15	52	

velocity values are ± 30%.

These results serve three functions.

1). They show that electrolyte velocity and the ensuing form drag on the bubbles attached to the surface are not the deciding factors in bubble separation, for if they were, the bubble separation diameter would increase as the current density is decreased, since the electrolyte velocity decreases.

2). It provides consistency with the dynamic theory of bubble separation presented above. Since the bubble growth rate is much slower at low current densities, the impact of neighboring bubbles hitting one another during growth may be only enough to separate them from the surface rather than causing coalescence. This would then result in a much smaller average bubble size than at higher current densities, where coalescence is more predominant.

3). It rules out the possibility that slight changes in electrode potential (lower current densities require less negative potentials) and their effect on the interfacial tension are decisive factors in determining bubble separation. On the negative branch of the electrocapillary curve a less negative potential results in a greater interfacial tension, which would result in larger bubbles, the opposite of the observed trend.

VI. CONCLUSIONS

The principal conclusions of this work can be summarized as follows:

1. The growth of gas bubbles on an electrode surface is a combination of growth by mass transfer of dissolved gas to the bubbles and coalescence of neighboring bubbles. Because of coalescence, the size of the bubbles on the surface and their number density are related, in that when the bubbles grow to a close-packed arrangement, coalescence between bubbles takes place, resulting in fewer but larger bubbles. Bubble dynamics before separation involves a series of such growth-coalescence sequences.
2. The growth characteristics of bubbles on the electrode surface are a strong function of the electrolyte's physical properties. The effect of electrode potential on these properties (namely the interfacial tension) results in different growth characteristics on the electrode surface for the same electrolyte at different electrode polarities.
3. In the range of gas generation rates 3.5-14 cm^3/cm^2 min, the nature of events is quite similar; the rates of bubble nucleation, growth, coalescence and separation increase linearly with current density.
4. Final bubble separation from the electrode surface at practical gas generation rates is controlled by the dynamics of the bubble interactions.
5. The microscopic roughness of a planar electrode has little effect on the character of gas evolution in the dynamic case.

6. Coalescence of rising bubbles in the turbulent stream well above the site of generation can be considerable. The degree of coalescence for a given electrolyte is primarily a function of gas generation rate, as related to the velocity field in the electrolyte.

REFERENCES

1. H. Y. Chen: Ph.D. Thesis, U. C. Berkeley, February 1967.
2. B. Kabanov and A. Frumkin, Z. fur Phys. Chem.: 165A, 433 (1933).
3. A. Coehn, Z. Elektrochem.: 29, 1 (1933).
4. A. Coehn and H. Neumann, Z. Physik: 20, 54 (1923).
5. H. Clark, P. Strenge, and J. W. Westwater, Chem. Engr. Progr. Symp. Ser.: 55, 103 (1959).
6. H. H. Kellogg, J. Electrochem. Soc.: 97, 133 (1950).
7. L. E. Scriven, Chem. Eng. Sci.: 10, 1 (1959).
8. D. E. Westerheide and J. W. Westwater, AICHE Journal: 7, 357 (1961).
9. N. Ibl, Chem. Ing. Techn.: 35, (1963).
10. J. P. Glas and J. W. Westwater, Int. J. Heat Mass Transfer: 7, 1427 (1964).
11. W. M. Buehl and J. W. Westwater, AICHE Journal: 12, 571 (1966).
12. D. Landolt, R. Acosta, R. Muller, and C. W. Tobias, J. Electrochem. Soc.: 117, 839 (1970).
13. C. K. Bon, Masters Thesis, U. C. Berkeley, Sept. 1970.
14. L. Janssen and Hoogland, Electrochim. Acta: 15, 1013 (1970).
15. L. Janssen and Hoogland, Electrochim. Acta: 18, 543 (1973).
16. N. Ibl and J. Venczel, Metalloberflache: 24, 367 (1970).
17. J. Venczel, Electrochim. Acta: 15, 1909 (1970).
18. N. Ibl, Chem. Ing. Techn.: 43, 202 (1971).
19. R. Darby and M. Haque, Chem. Eng. Sci.: 28, 1129 (1973).
20. D. W. Moore, Journal of Fluid Mechanics: 6, 113 (1959).
21. I. Rousar, J. Electrochem. Soc.: 116, 676 (1969).

22. T. K. Sherwood, R. L. Pigford, and C. R. Wilke, Mass Transfer: McGraw-Hill, New York (to be published).

23. M. Eisenberg, C. W. Tobias, and C. R. Wilke, J. Electrochem. Soc.: 102, 415 (1955).

24. J. T. Davies and E. K. Rideal, Interfacial Phenomena: Academic Press, New York (1963).

25. R. D. Walker, Sixth Semi-Annual Report, February 1969, NASA Research Grant NGR 10-005-022.

ACKNOWLEDGMENTS

This work was supported by the U. S. Energy Research and Development Administration.

TECHNICAL INFORMATION DIVISION
LAWRENCE BERKELEY LABORATORY
UNIVERSITY OF CALIFORNIA
BERKELEY, CALIFORNIA 94720